RESTRICTED UNCLASSIFIED

COPY NO. 4

RM No. E7F10

NACA

AUG 20 1947

RESEARCH MEMORANDUM

ALTITUDE-WIND-TUNNEL INVESTIGATION OF THRUST AUGMENTATION OF A TURBOJET ENGINE

III - PERFORMANCE WITH TAIL-PIPE BURNING IN STANDARD-SIZE TAIL PIPE

By William A. Fleming and Richard L. Golladay

Flight Propulsion Research Laboratory
Cleveland, Ohio

CLASSIFIED DOCUMENT

This document contains classified information affecting the National Defense of the United States within the meaning of the Espionage Act, USC 50:31 and 32. Its transmission or the revelation of its contents in any manner to an unauthorized person is prohibited by law. Information so classified may be imparted only to persons in the military and naval Services of the United States, appropriate civilian officers and employees of the Federal Government who have a legitimate interest therein, and to United States citizens of known loyalty and discretion who of necessity must be informed thereof.

TECHNICAL EDITING WAIVED

NATIONAL ADVISORY COMMITTEE FOR AERONAUTICS

WASHINGTON

August 11, 1947

RESTRICTED

NATIONAL ADVISORY COMMITTEE FOR AERONAUTICS

RESEARCH MEMORANDUM

ALTITUDE-WIND-TUNNEL INVESTIGATION OF THRUST AUGMENTATION OF A TURBOJET ENGINE

III - PERFORMANCE WITH TAIL-PIPE BURNING IN STANDARD-SIZE TAIL PIPE

By William A. Fleming and Richard L. Golladay

SUMMARY

Thrust augmentation of a turbojet engine by burning fuel in the tail pipe has been investigated in the NACA Cleveland altitude wind tunnel. The engine performance was determined at several simulated flight conditions throughout a range of tail-pipe fuel flows. A tail-pipe combustion chamber having the same external dimensions as the standard turbojet-engine tail pipe was investigated to determine whether satisfactory operation could be obtained at high-speed and high-altitude flight conditions. Comparisons are made of the performance data obtained with two different flame holders installed in this tail pipe, with a tail pipe 34 inches in diameter, and with values calculated assuming no pressure loss across the tail pipe.

At a simulated altitude of 20,000 feet and a flight Mach number of 0.8, the net thrust of the engine was increased 76 percent with the standard-size tail-pipe combustion chamber and turning-vane flame holder. At 30,000 feet altitude and a flight Mach number of 0.9, the net thrust was increased 59 percent with the standard-size tail-pipe combustion chamber and a conical-grid flame holder, whereas at the same simulated flight conditions the net thrust was increased 103 percent with a 34-inch diameter tail-pipe combustion chamber. A portion of these increases in thrust were due to the fact that the turbine-outlet temperature at rated engine speed with the standard tail pipe and tail-pipe nozzle was below the limiting value whereas with tail-pipe burning the turbine-outlet temperature was at the limiting value.

The pressure loss across the standard-size tail-pipe combustion chamber was greater than across the large one. The combustion efficiency was lower with the standard-size tail-pipe

combustion chamber than with the large one. Excessively high tail-pipe shell temperatures were observed with each of the flame holders installed in the standard-size tail pipe during operation at a tail-pipe fuel-air ratio sufficiently high to give limiting turbine-outlet temperature at maximum engine speed.

INTRODUCTION

Thrust augmentation is of extreme importance for increasing the range of application of turbojet engines. The burning of fuel in the tail pipe provides a practical cycle for increasing the thrust of the turbojet engine without increasing the temperature or stresses in the turbine buckets or otherwise disturbing the cycle of engine operation, provided that the tail pipe is equipped with an adjustable-area nozzle.

As part of a general program on thrust augmentation of turbojet engines conducted at the NACA Cleveland laboratory, an investigation was made in the altitude wind tunnel on an axial-flow compressor-type turbojet engine to determine the feasibility of using a tail-pipe combustion chamber that has the same external dimensions as the standard engine tail pipe. Evaluation of tail-pipe burning in this engine with a larger tail-pipe combustion chamber is discussed in reference 1. Results of investigations on tail-pipe burning in this engine at static sea-level conditions are presented in reference 2. An investigation of thrust augmentation by means of injecting water at the inlet of an axial-flow compressor engine is discussed in reference 3.

The most important characteristics of an efficient tail-pipe burner are:

1. Maximum thrust at high over-all efficiency

2. Wide range of stable burner operation

3. Minimum thrust loss for operation without tail-pipe burning

4. Minimum increase in over-all dimensions of engine

5. Adequate tail-pipe cooling

6. Light weight

In the obtainment of these characteristics numerous research problems are introduced. The investigation of reference 1 was directed at the first two characteristics with little regard for size or weight of the installation. The present investigation had the same objectives with the additional consideration of minimum changes in the physical size of the turbojet engine.

Operational characteristics of seven flame holders were obtained over a range of simulated flight conditions. A 21-inch-diameter tail-pipe nozzle was used in the engine with each flame holder. Performance data obtained with the two best flame holders are presented for simulated altitudes of 20,000 and 30,000 feet and ram-pressure ratios from 1.19 to 1.98. These results are compared with the experimental results presented in reference 1 and with theoretical calculations, which were made assuming no losses across the tail pipe. In the following sections of this report, the standard-size tail-pipe combustion chamber is referred to as the "small tail pipe" and the 34-inch diameter combustion chamber discussed in reference 1 is referred to as the "large tail pipe."

FUNDAMENTALS OF TAIL-PIPE BURNING

The jet thrust of a turbojet engine is equal to the product of the mass rate of gas flow and the jet velocity. Thrust augmentation of a turbojet engine by burning fuel in the tail-pipe combustion chamber results in an increase of the final jet velocity. The value of the final jet velocity is given by

$$V_j = M_j \sqrt{\gamma_j g R t_j} \tag{1}$$

and the Mach number of the jet is

$$M_j = \sqrt{\frac{2}{\gamma_j - 1}\left[\left(\frac{P_j}{p_0}\right)^{\frac{\gamma_j - 1}{\gamma_j}} - 1\right]} \tag{2}$$

For convenience, all symbols are defined in appendix A.

Equation (1) indicates that the jet velocity, and therefore the jet thrust, is proportional to the jet Mach number and the square root of the static jet temperature. Maximum jet temperature is reached when sufficient fuel is added in the engine and the tail pipe to burn completely all the oxygen in the air passing through the engine. The jet Mach number M_j is principally a function of the pressure ratio P_j/p_0 (equation (2)), which remains essentially constant at fixed engine and flight conditions, and is independent of the jet temperature except for determining the value of γ. Maximum pressure ratio is obtained when the engine is operated at the maximum allowable engine speed and turbine-outlet temperature.

As the amount of fuel burned in the tail pipe is varied, the tail-pipe-nozzle area must be changed to maintain maximum allowable engine conditions. An expression for jet thrust involving jet area and jet Mach number is

$$F_j = \gamma_j p_0 A_j M_j^2 \tag{3}$$

Because the jet thrust at fixed engine operating conditions is proportional to the square root of the jet temperature, the jet area required to maintain maximum allowable turbine-outlet temperature at maximum engine speed is proportional to the square root of the jet temperature.

WIND-TUNNEL INSTALLATION AND PROCEDURE

The TG-180 engine has an 11-stage axial-flow compressor, eight cylindrical combustion chambers, a single-stage turbine, a tail pipe, and an exhaust nozzle. The over-all length of the standard engine is 14 feet and the maximum diameter is 36 inches.

A standard TG-180 turbojet engine without cowling was suspended from a wing section installed in the 20-foot-diameter test section of the altitude wind tunnel. Refrigerated air was supplied to the engine through a duct from the tunnel make-up system. A labyrinth seal in this duct located 40 feet upstream of the engine inlet made possible the measurement of thrust with the tunnel-balance scale system. The air was throttled from approximately sea-level pressure to the desired pressure at the engine inlet while the pressure in the wind-tunnel test section was maintained at the desired altitude. The temperature of the engine-inlet air was regulated to the approximate NACA standard temperature corresponding to the simulated flight speed and altitude.

Preliminary calibration runs were made with the engine equipped with a standard-size tail-pipe nozzle, which was $16\frac{3}{4}$ inches in diameter, to provide a basis for evaluating changes in performance resulting from tail-pipe burning.

Operational characteristics of seven flame holders were studied at simulated altitudes from 5000 to 30,000 feet and ram-pressure ratios from 1.05 to 1.98. Performance data are presented for the two most satisfactory flame holders investigated. Engine performance data are presented for the one flame holder at a simulated altitude of 20,000 feet and ram-pressure ratios of 1.19 and 1.54 and for the other flame holder at a simulated altitude of 30,000 feet and ram-pressure ratios of 1.67 and 1.98.

At each simulated flight condition, the engine was operated at a speed of 7600 rpm and data were obtained at various tail-pipe fuel flows. The minimum fuel flow was determined by combustion blow-out in the tail pipe and the maximum fuel flow was determined by limiting turbine-discharge temperature (1680° R). A large tail-pipe nozzle of 21-inch diameter was used to permit high fuel flows for the tail-pipe burning without exceeding the maximum turbine-discharge temperature.

A survey rake was mounted in the inlet duct $11\frac{1}{4}$ feet upstream of the engine inlet to measure the engine air flow. Pressures and temperatures of the gases were measured at seven stations in the engine (fig. 1). A tail-pipe rake was so mounted at station 7 that it could be retracted from the nozzle outlet. Measurements were made with this rake only for conditions with no tail-pipe burning because of the high gas temperatures obtained when fuel was burning in the tail pipe. Thrust was determined from the balance scales for all the test conditions for which data are presented. The methods used to determine thrust and air flow from these measurements are given in appendix A.

Kerosene (AN-F-32) was burned in the engine and 62-octane unleaded gasoline was burned in the tail-pipe combustion chamber. The fuel flows to the engine and the tail pipe were measured by calibrated rotameters.

DESCRIPTION AND OPERATING CHARACTERISTICS OF FLAME-HOLDER INSTALLATIONS

A tail-pipe combustion chamber having the same external dimensions as the standard engine tail pipe was installed. The standard tail pipe has an inside diameter of 34 inches at the front flange, 21 inches at the rear flange, and is $58\frac{3}{4}$ inches long. The inner cone of the tail pipe was shortened to provide space for installation of the seven flame holders investigated. A sketch of the engine and the tail-pipe combustion chamber without a flame holder and the position at which the flame holders were installed are shown in figure 1. Fuel was injected through spray bars at manifold pressures from 5 to 175 pounds per square inch. Downstream of the flame holder the tail pipe was wrapped with 0.75-inch diameter copper tubing through which water was circulated to cool the shell. A 21-inch diameter tail-pipe nozzle was used, which was constructed by seam-welding a corrugated outer shell to a smooth inner shell in such a way that a helical cooling-water path was formed.

Flame holder A. - The first flame holder investigated (flame holder A) was constructed of horizontal and vertical V-type gutters with the vertex of the gutters directed upstream (fig. 2). These gutters had an included angle of 30°, were 1-inch across the open end, and were spaced on $2\frac{1}{2}$-inch center lines. This flame holder is similar in design to the one used in the large tail pipe, which is described in reference 1. In order to accommodate the flame holder, the inner cone of the tail pipe was revised as shown by the dashed section in figure 1. The flame holder was 28 inches in diameter and was installed 27 inches downstream of the turbine. Liquid fuel was injected normal to the direction of gas flow through small holes in five horizontal spray bars attached to the vertex of alternate horizontal gutters. The fuel was ignited by means of propane blown over a spark plug. This flame holder restricted the flow in the tail pipe to such an extent that the tail-pipe temperature was very near the limiting value at maximum engine speed with no tail-pipe burning. Operation with this flame holder was therefore limited to low fuel-air ratios in order not to exceed the limiting turbine-outlet temperature. The flame blew out at maximum engine speed, an altitude of 5000 feet, and a ram-pressure ratio of approximately 1.05. Combustion blow-out was apparently caused by the high velocity of the gas through the flame holder.

Flame holder B. - Because improved combustion was believed possible with larger gutters, a variation of flame holder A (flame holder B) was investigated, which also had horizontal and vertical V-type gutters. The gutters on flame holder B maintained the included angle of 30° but were 2 inches across the open end and were spaced on 5-inch center lines (fig. 3). The location of this flame holder in the tail pipe and the method of fuel injection were the same as for flame holder A. Combustion was so improved that tail-pipe burning could be maintained at full engine speed. The flame holder, however, still blocked the tail pipe to such an extent that excessively high turbine-outlet temperatures were obtained with low tail-pipe fuel-air ratios at maximum engine speed, an altitude of 5000 feet, and a ram-pressure ratio of approximately 1.05.

Flame holder C. - Flame holder C was then designed having three circumferential turning vanes that diffused the gas by turning it toward the center of the tail pipe and into a conical grid of V-type gutters (fig. 4). The principle of this design was to lower the gas velocity by turning the air into a conical section of greater area than the cross section of the tail pipe. In order to accommodate this flame holder, the inner cone of the tail pipe was removed and a spherical dome (fig. 5) was attached to the inner cone at a point 16 inches downstream of the turbine. The location of the dome in the tail pipe is shown in figure 4. Fuel was injected normal to the direction of gas flow through eight equally spaced radial spray bars installed approximately 3 inches downstream of the turbine. A pilot used only for igniting the fuel was installed at the center of the dome as shown in figure 5. The ignition pilot consisted of a cylinder fitted with a perforated conical liner, a fuel spray nozzle, and two spark plugs. Compressed air for burning was supplied to the pilot from an external source during the time the fuel in the tail pipe was being ignited.

Combustion was more stable with flame holder C than with any of the others investigated. After short periods of tail-pipe burning, however, sections of flame holder C were burned away. Some burning evidently occurred before the gas passed through the flame holder. Burning was maintained at tail-pipe fuel-air ratios between 0.022 and 0.027 at maximum engine speed, a simulated altitude of 30,000 feet, and a ram-pressure ratio of 1.98. The maximum fuel-air ratio presented for all the flame holders was limited by the maximum allowable turbine-outlet temperature. The flame holders could have been investigated at higher fuel-air ratios if a larger tail-pipe nozzle had been used. Performance data obtained with flame holder C are presented.

Flame holder D. - In order to determine whether the turning vanes alone would hold the flame, the conical grid was removed and the same fuel-injection system was used. With a flame holder of only turning vanes (flame holder D), combustion was unstable at high altitudes and high engine speeds. The flame blew out immediately after the fuel was ignited at an altitude of 20,000 feet and an engine speed of about 4000 rpm. Combustion in the tail pipe was stable at an altitude of 5000 feet and at maximum engine speed.

Flame holder E. - The turning vanes were then modified by welding a section around the inside of the vanes near the trailing edge to form a V-type gutter (flame holder E). (See fig. 6.) The gutter had an included angle of 15° and was 3/4 inch across the open end. The combustion characteristics were slightly better with flame holder E than with the turning vanes alone (flame holder D). The flame blew out as soon as the fuel was ignited at an altitude of 30,000 feet. At an altitude of 20,000 feet and a ram-pressure ratio of approximately 1.10, the flame blew out at an engine speed slightly above 6500 rpm with a tail-pipe fuel-air ratio of 0.029. Combustion was stable at an altitude of 5000 feet and maximum engine speed.

Flame holder F. - A further modification of the turning vanes was made by welding a section similar to the one welded on flame holder E on the outside of the vanes near the trailing edge to increase the size of the gutter, flame holder F (fig. 7). The gutter then had an included angle of 30° and was $1\frac{1}{2}$ inches across the open end. With the guide vanes modified in this manner, burning was maintained in the tail pipe at altitudes up to 30,000 feet and at maximum engine speed. No investigation was made at a higher altitude. A maximum tail-pipe fuel-air ratio of 0.027 was obtained at a simulated altitude of 30,000 feet and a ram-pressure ratio of 2.00. Available equipment limited further operation with flame holder F to an altitude of 20,000 feet. At 20,000 feet and maximum engine speed, tail-pipe fuel-air ratios from 0.024 to 0.035 were obtained at a ram-pressure ratio of 1.19 and fuel-air ratios from 0.020 to 0.029 were obtained at a ram-pressure ratio of 1.54. Combustion was nearly as stable with this flame holder as with the flame holder having turning vanes and the conical grid of V-type gutters. Inspection of flame holder F after operation revealed that the gutters at the trailing edge of the turning vanes had been excessively hot, but no portion of the flame holder had been burned away. Performance data obtained with flame holder F are presented.

Flame holder G. - The last flame holder investigated was a perforated conical section installed in the tail pipe with the apex downstream (fig. 8). The diameter of flame holder G at the upstream end was $26\frac{1}{2}$ inches, at the downstream end $4\frac{1}{8}$ inches, and the length was 19 inches. Flame holder G was installed $19\frac{1}{2}$ inches downstream of the turbine and a gap of $1\frac{5}{8}$ inches was left between the cone and the wall of the tail pipe. Holes approximately 1 inch in diameter were punched in the flame holder as close together as practicable and still maintain sufficient structural strength. Separate investigations were made with the eight radial fuel spray bars located at different positions. In one case the spray bars were located 3 inches and the other case $13\frac{1}{2}$ inches downstream of the turbine. The perforated cone held the flame for only a short time after maximum engine speed was reached at a simulated altitude of 5000 feet. Combustion in the tail pipe at an altitude of 20,000 feet was not possible at engine speeds above 5000 rpm. Changes in the location of the spray bars had no noticeable effect on combustion.

General operating characteristics. - With all seven flame holders investigated apparently considerable fuel was burned near the wall of the tail pipe. During operation at tail-pipe fuel-air ratios sufficiently high to give limiting turbine-outlet temperature at maximum engine speed, the shell of the tail pipe was excessively hot even though it was wrapped with cooling coils.

Fuel could not be ignited in the tail pipe at engine speeds above 4500 rpm with any of the flame holders investigated and in some cases it was necessary to reduce the engine speed to 3500 rpm before the fuel would ignite. An engine speed limit for ignition of 4500 rpm was also encountered in the investigations reported in reference 1 with the large tail-pipe combustion chamber.

Because no high-voltage insulation was available that could withstand temperatures up to 1200°F, the wires running through the inner cone to the spark plugs in the ignition pilot usually shorted out after the engine had been operating for a short period of time. In order to ignite the tail-pipe fuel after the wires were shorted out, it was necessary to accelerate the engine rapidly, thereby obtaining a burst of flame through the turbine and into the tail pipe.

PERFORMANCE WITH TAIL-PIPE BURNING

Data obtained at an altitude of 20,000 feet and ram-pressure ratios of 1.19 and 1.54 with flame holder F, consisting of the three turning vanes and the $1\frac{1}{2}$-inch gutters welded to the trailing edge (fig. 7), are presented in figure 9. Data obtained at 30,000 feet and ram-pressure ratios of 1.67 and 1.98 with flame holder C, consisting of the conical grid of V-type gutters (fig. 4), are shown in figure 10.

Figures 9 and 10 present (a) jet thrust, (b) net thrust, (c) engine fuel consumption, (d) specific fuel consumption based on net thrust, (e) air flow, (f) total fuel-air ratio, and (g) tail-pipe total-pressure ratio as functions of tail-pipe fuel consumption. A limit line is drawn on the figures to indicate the conditions at which maximum allowable turbine-outlet temperature (1680° R) was obtained. The total fuel-air ratios (figs. 9(f) and 10(f)) were considerably below the stoichiometric limit of 0.067. Operation of the small tail-pipe combustion chamber with flame holders C and F would therefore be desirable with a tail-pipe nozzle larger than the one used because more thrust could then be obtained from the engine at limiting turbine-outlet temperature provided the pressure losses in the tail pipe were not too great.

At rated engine speed with the standard tail pipe and nozzle, the engine operated at approximately limiting tail-pipe temperatures at low-altitude and low-airspeed conditions. At 30,000 feet altitude and at the high ram-pressure ratios at which the investigations were conducted, the tail-pipe temperature was lower than the maximum allowable temperature. A variable-area nozzle should be used to maintain limiting temperature. Because present installations of turbojet engines do not use a variable-area nozzle, the results of the tail-pipe burning investigation have been compared with the engine using a standard nozzle with a fixed diameter of $16\frac{3}{4}$ inches.

The significant results of this investigation were obtained at conditions where the turbine-outlet temperature reached the limiting value of 1680° R, as indicated by the dashed lines in figures 9 and 10. The succeeding discussion is confined to the results obtained at these conditions.

Comparisons between the data obtained with flame holders C and F in the small combustion chamber and the data presented in reference 1 with the large combustion chamber are shown in

figures 11 to 16. Variations in corrected jet thrust with tail-pipe total-pressure ratio for the small tail-pipe combustion chamber at altitudes of 20,000 and 30,000 feet and with a 21-inch-diameter tail-pipe nozzle on the engine are shown in figure 11 for maximum engine speed and for all of the data shown in figures 9 and 10. Data are also presented for the large tail-pipe combustion chamber at an altitude of 30,000 feet with a 21-inch-diameter tail-pipe nozzle. These data are corrected to sea-level conditions in order to facilitate comparison between the results obtained at 20,000 and 30,000 feet. A curve showing the corrected jet thrust obtainable with no total-pressure loss in the tail pipe is also presented in figure 11. This curve was calculated by means of equations (2) and (3). Throughout the range of tail-pipe total-pressure ratios investigated, the corrected jet thrust with the small tail-pipe combustion chamber and flame holder C was approximately 30 percent less than the thrust calculated for no pressure loss across the tail pipe and 14 percent less than the thrust obtained with the large tail-pipe combustion chamber (reference 1). With the small tail-pipe combustion chamber and flame holder F, the corrected jet thrust was approximately 26 percent lower than the thrust calculated for no pressure loss across the tail pipe and 5 percent lower than the thrust with the large tail pipe.

The differences in thrust shown in figure 11 are attributed to friction and to combustion pressure losses in the tail pipe. The friction loss across flame holder F amounted to about 9 percent of the turbine-outlet total pressure, whereas the friction loss with the large tail-pipe combustion chamber was about 7 percent of the turbine-outlet total pressure. The friction pressure loss was not measured across flame holder C. As indicated in figure 11, however, the greatest pressure loss occurred with the small tail-pipe combustion chamber and flame holders C and F.

The relation among tail-pipe total-temperature ratio, tail-pipe-nozzle-outlet total temperature, and tail-pipe fuel-air ratio at limiting turbine-outlet temperature is shown in figure 12 for the large and the small tail-pipe combustion chambers. The dashed line shows the theoretical total-temperature ratio calculated assuming 100-percent combustion efficiency, a heating value of the fuel equal to 19,000 Btu per pound, and no dissociation. The calculated total-temperature ratio increased very nearly linearly with the fuel-air ratio, and the departure from a linear variation is caused by the variation in the specific heat of the gas with gas temperature. The values of total temperature were calculated with equation (B5) of appendix B using experimental values of jet thrust and gas flow. Tail-pipe-nozzle-outlet temperatures up to 2865° R were obtained with

flame holder C and temperatures up to 2620° R were obtained with flame holder F. These temperatures are somewhat lower than the temperature of 3360° R obtained with the large tail-pipe combustion chamber. A larger nozzle on the small tail pipe would permit higher total fuel-air ratios and thus correspondingly higher tail-pipe temperatures.

Tail-pipe combustion efficiency was computed by equation (A7) in appendix A using the calculated values of tail-pipe temperature shown in figure 12. Tail-pipe combustion efficiency is presented in figure 13 as a function of tail-pipe total pressure. The pressure is the most important variable affecting combustion efficiency in this case inasmuch as the Mach number and the temperature at the flame-holder inlet were approximately the same for each of the conditions presented in figure 13 and the tail-pipe fuel-air ratio did not differ greatly among these conditions. With each tail pipe, the combustion efficiency increased as the tail-pipe total pressure became higher, that is, with increases in flight Mach number. The combustion efficiency was lower with the small tail pipe than with the large one throughout the range investigated. For example, at a tail-pipe total pressure of 2400 pounds per square foot absolute, the combustion efficiency was 65.5 percent for flame holder F, 67 percent for flame holder C, and 79.5 percent for the large tail-pipe combustion chamber.

Measured values of net thrust obtained at an altitude of 20,000 feet for the engine with a standard engine tail pipe with a $16\frac{3}{4}$-inch-diameter nozzle and for the small tail-pipe combustion chamber with flame holder F are shown in figure 14(a). The net thrust obtained at a pressure altitude of 30,000 feet for the engine with a standard tail pipe and $16\frac{3}{4}$-inch-diameter tail-pipe nozzle, for the small tail-pipe combustion chamber with flame holder C, and for the large tail-pipe combustion chamber are shown in figure 14(b). The values given for tail-pipe burning were obtained with a 21-inch-diameter tail-pipe nozzle and a limiting temperature of 1680° R at the turbine outlet, whereas with the standard tail pipe the turbine-outlet temperature was 1530° R. A portion of the increase in thrust shown in figure 14 is due to this difference in turbine-outlet temperatures. The values of thrust given for the engine with the standard tail pipe at an altitude of 20,000 feet (fig. 14(a)) were generalized to this altitude from performance data obtained at 30,000 feet.

These values of thrust were used in figure 15 to obtain the percentage increase in net thrust attributable to the three tail-pipe configurations. At an altitude of 20,000 feet and an

equivalent flight Mach number of 0.8, the net thrust was increased 76 percent with the small tail-pipe combustion chamber and flame holder F as compared to 100 percent at an altitude of 30,000 feet with the large tail-pipe combustion chamber. At an altitude of 30,000 feet and an equivalent Mach number of 0.9, the net thrust was increased 59 percent with the small tail-pipe combustion chamber and flame holder C as compared to 103 percent with the large tail-pipe combustion chamber. The differences in thrust between the small and the large tail-pipe combustion chambers is attributed to higher internal losses and lower tail-pipe temperature ratios for the small tail pipe. Higher internal losses were incurred with flame holder C than with flame holder F in the small tail pipe, which accounts for the lower thrusts obtained. Therefore, at each flight condition, the total fuel-air ratio at which limiting turbine-outlet temperatures were obtained decreased as the losses across the tail pipes became greater, as shown in figure 16. The total-temperature ratio across the tail pipe remains essentially constant with changes in flight Mach number (fig. 12) and the combustion efficiency increases with flight Mach number (fig. 13); therefore, the decrease in total fuel-air ratio as the flight Mach number is raised is mainly the result of changes in combustion efficiency.

Specific fuel consumptions based on net thrust that correspond to the thrust results of figures 14(a) and 14(b) are shown in figures 17(a) and 17(b), respectively. At a flight Mach number of 0.8 and an altitude of 20,000 feet, the specific fuel consumption with the small tail pipe and flame holder F was 79 percent higher than with the standard engine and tail pipe (fig. 17(a)). At a flight Mach number of 0.9 and an altitude of 30,000 feet, the specific fuel consumption increased 77 percent for the small tail pipe with flame holder C as compared to 80 percent for the large tail pipe (fig. 17(b)). The efficiency of a tail-pipe burning cycle is lower than that of a turbojet-engine cycle. Therefore, at any fixed engine condition the efficiency of the combined cycles decreases as the amount of tail-pipe burning is increased. Higher pressure losses in the small tail pipe so lowered the efficiency that the specific fuel consumption was about the same for the large and the small tail-pipe combustion chambers.

SUMMARY OF RESULTS

The following results were obtained from an investigation of a tail-pipe combustion chamber having the same external dimensions as the standard tail pipe at altitudes of 20,000 and 30,000 feet and ram-pressure ratios from 1.19 to 1.98:

1. At an altitude of 20,000 feet and an equivalent flight Mach number of 0.8, the net thrust was increased 76 percent with the small tail-pipe combustion chamber and flame holder F consisting of turning vanes with a V-type gutter at the trailing edges. The corresponding specific fuel consumption based on net thrust was increased 79 percent. At an altitude of 30,000 feet and a flight Mach number of 0.9, the net thrust was increased 59 percent with the small tail-pipe combustion chamber and flame holder C consisting of turning vanes and a conical grid of V-type gutters, whereas the net thrust was increased 103 percent with the large tail-pipe combustion chamber. The corresponding increases in specific fuel consumption based on net thrust were 77 and 80 percent. A portion of this increase in thrust was due to the fact that the turbine-outlet temperature at rated engine speed with the standard tail pipe and tail-pipe nozzle was below the limiting value.

2. As a result of higher pressure losses in the small tail-pipe combustion chamber, the corrected jet thrust with the small tail-pipe combustion chamber and flame holder C was approximately 30 percent less than the thrust calculated assuming no pressure loss across the tail pipe and 14 percent less than the thrust obtained with the large tail-pipe combustion chamber. With flame holder F, the corrected jet thrust was approximately 26 percent lower than the theoretical thrust and 5 percent lower than the thrust obtained with the large tail pipe.

3. The combustion efficiency was lower with the small tail-pipe combustion chamber than with the large one. At a tail-pipe total pressure of 2400 pounds per square foot absolute, the combustion efficiency was 79.5 percent for the large tail pipe, 67 percent for flame holder C in the small tail pipe, and 65.5 percent for flame holder F in the small tail pipe.

4. The most stable combustion was obtained in the small tail pipe with flame holder C. After short periods of tail-pipe burning, however, sections of this flame holder were burned away.

5. Excessively high tail-pipe shell temperatures were observed with each of the seven flame holders installed in the

small tail pipe during operation at a tail-pipe fuel-air ratio sufficiently high to give limiting turbine-outlet temperature at maximum engine speed.

Flight Propulsion Research Laboratory,
National Advisory Committee for Aeronautics,
Cleveland, Ohio.

APPENDIX A

METHODS OF CALCULATION

Symbols

The following symbols are used in the calculations:

A	cross-sectional area, sq ft
a	speed of sound, ft/sec
B	thrust scale reading, lb
C_D	external drag coefficient of installation (determined from power-off tests)
c_p	specific heat of gas at constant pressure, Btu/(lb)($^\circ$F)
F_j	jet thrust, lb
F_n	net thrust, lb
g	acceleration of gravity, ft/sec^2
H	enthalpy, Btu/lb
h_c	lower heating value of fuel, Btu/lb
J	mechanical equivalent of heat, ft-lb/Btu
M	Mach number
P	total pressure, lb/sq ft absolute
P_1/p_0	ram-pressure ratio
p	static pressure, lb/sq ft absolute
q	dynamic pressure, lb/sq ft
R	universal gas constant, ft-lb/(lb)($^\circ$F)
S	wing-section area, sq ft
T	total temperature, $^\circ$R

T_i indicated temperature, °R

t static temperature, °R

V velocity, ft/sec

W_a air flow, lb/sec

W_f total fuel consumption, lb/hr

$W_{f,e}$ turbojet-engine fuel consumption, lb/hr

$W_{f,t}$ tail-pipe fuel consumption, lb/hr

W_g exhaust gas flow, lb/sec

W_f/F_n specific fuel consumption based on total fuel consumption and net thrust, lb/(hr)(lb thrust)

f/a fuel-air ratio based on total fuel flow to engine and tail pipe

δ ratio of free-stream static pressure to static pressure at NACA standard atmospheric conditions, $p_0/2116$

η_b tail-pipe combustion efficiency, percent

γ ratio of specific heats of gases

ρ mass density of gas, slugs/cu ft

τ total-temperature ratio across tail pipe, T_7/T_6

Subscripts:

f fuel

j station at which static pressure of jet reaches free-stream ambient pressure

r inlet duct at survey rake, station r

t tail pipe

x inlet duct at slip joint, station x

0	tunnel test-section free-air stream
1	cowl inlet
6	diffuser inlet
7	tail-pipe-nozzle outlet

Temperature

A cold calibration of a sample thermocouple to a Mach number of about 0.8 showed that the thermocouple measured the static temperature plus approximately 85 percent of the adiabatic temperature rise owing to the impact of the air on the thermocouple. Static temperature was determined from indicated temperature when this factor was applied to the adiabatic relation between temperature and pressure in the following manner:

$$t = \frac{T_i}{1 + 0.85\left[\left(\frac{P}{p}\right)^{\frac{\gamma-1}{\gamma}} - 1\right]} \tag{A1}$$

The total temperature was determined from

$$T = t\left(\frac{P}{p}\right)^{\frac{\gamma-1}{\gamma}} = \frac{T_i\left(\frac{P}{p}\right)^{\frac{\gamma-1}{\gamma}}}{1 + 0.85\left[\left(\frac{P}{p}\right)^{\frac{\gamma-1}{\gamma}} - 1\right]} \tag{A2}$$

Air Flow

The air flow through the engine was determined from pressure and temperature measurements obtained with a vertical survey rake installed in the inlet duct $11\frac{1}{4}$ feet ahead of the engine inlet. Air flow was calculated by

$$W_a = \rho_r A_r V_r g = \frac{p_r A_r}{R} \sqrt{\frac{2Jgc_p}{t_r} \left[\left(\frac{p_r}{p_r} \right)^{\frac{\gamma-1}{\gamma}} - 1 \right]} \qquad (A3)$$

The static temperature in equation (A3) was obtained by use of equation (A1).

Jet Thrust

Jet thrust was determined from the balance-scale measurements by combining the forces on the installation in the following equation:

$$F_j = B + C_D q_0 S + \frac{W_a V_x}{g} + A_x(p_x - p_0) \qquad (A4)$$

The second term in the right-hand side of equation (A4) represents the external drag of the installation and the third and fourth terms combined represent the force on the installation at the frictionless slip joint in the inlet-air duct.

Equivalent Airspeed

Inasmuch as all calculations are based on 100-percent ram recovery, the equivalent airspeed corresponding to the ram-pressure ratio at the engine inlet can be expressed by

$$V_0 = \sqrt{2Jgc_p T_{i,1} \left[1 - \left(\frac{p_0}{p_1} \right)^{\frac{\gamma-1}{\gamma}} \right]} \qquad (A5)$$

Because the adiabatic temperature rise due to the cowl-inlet velocity was low, the equivalent free-stream total temperature was assumed equal to the cowl-inlet indicated temperature. The use of this assumption introduced an error in airspeed of less than 1 percent.

Net Thrust

When equations (A3), (A4), and (A5) are combined, the equivalent free-stream momentum of the inlet air may be subtracted from the jet thrust and the following equation for net thrust is obtained:

$$F_n = F_j - \frac{W_a V_0}{g} \tag{A6}$$

Combustion Efficiency

The tail-pipe combustion efficiency was obtained by dividing the heat added in the tail pipe by the heat content of the fuel supplied.

$$\eta_b = \frac{3600\, W_{g,7}\, c_{p,7}\, T_7 - 3600\, W_{g,6}\, c_{p,6}\, T_6 - W_{f,t}\, H_{f,t}}{h_{c,t}\, W_{f,t}} \tag{A7}$$

The numerator of the right-hand side of this equation is composed of the total heat in the gas leaving the tail pipe, the total heat in the gas entering the tail pipe, and the initial heat in the liquid fuel added in the tail pipe.

Integrated values of c_p that took into account the effect of temperature and fuel-air ratio were used. Dissociation of the gases at high temperatures was disregarded. The heating value of the fuel used was 19,000 Btu per pound.

APPENDIX B

DERIVATION OF EQUATION FOR ESTIMATING GAS TEMPERATURES FROM THRUST AND GAS FLOW

In all the cases reported, the jet velocity was supersonic. It is therefore assumed that sonic velocity exists at the outlet of the tail-pipe nozzle, station 7. The jet thrust F_j is given by

$$F_j = \frac{W_g}{g} V_7 + A_7(p_7 - p_0)$$

The velocity V_7 equals the sonic velocity a_7; consequently,

$$F_j = \frac{W_g}{g} a_7 + A_7(p_7 - p_0) \tag{B1}$$

The pressure p_7 at the nozzle outlet can be eliminated by the equation of continuity

$$W_g = \rho_7 A_7 V_7 g$$
$$= \frac{\gamma_7 p_7 A_7 g}{a_7} M_7$$

But $M_7 = 1.0$; therefore

$$p_7 = \frac{W_g a_7}{\gamma_7 A_7 g}$$

Equation (B1) can then be reduced to

$$F_j = \frac{W_g a_7}{g} \left(1 + \frac{1}{\gamma_7}\right) - A_7 p_0$$

Solving for a_7,

$$a_7 = \frac{F_j + p_0 A_7}{W_g} \left(\frac{\gamma_7}{\gamma_7+1}\right) \tag{B2}$$

The static temperature at station 7 is related to a_7 by

$$t_7 = \frac{a_7^2}{\gamma_7 R} \tag{B3}$$

and the relation of total to static temperature at station 7, where M = 1.0, is

$$\frac{T}{t} = 1 + \frac{\gamma-1}{2} = \frac{1+\gamma}{2} \tag{B4}$$

When equations (B2), (B3), and (B4) are combined, the following expression for the total temperature T_7 is obtained:

$$T_7 = \frac{\gamma_7(F_j + p_0 A_7)^2}{2R W_g^2(\gamma_7 + 1)} \tag{B5}$$

REFERENCES

1. Fleming, W. A., and Dietz, R. O.: Altitude-Wind-Tunnel Investigations of Thrust Augmentation of a Turbojet Engine. I - Performance with Tail-Pipe Burning. NACA RM No. E6I20, 1946.

2. Lundin, Bruce T., Dowman, Harry W., and Gabriel, David S.: Experimental Investigation of Thrust Augmentation of a Turbojet Engine at Zero Ram by Means of Tail-Pipe Burning. NACA RM No. E6J21, 1946.

3. Dietz, Robert O., and Fleming, William A.: Altitude-Wind-Tunnel Investigation of Thrust Augmentation of a Turbojet Engine. II - Performance with Water Injection at Compressor Inlet. NACA RM No. E7C12, 1947.

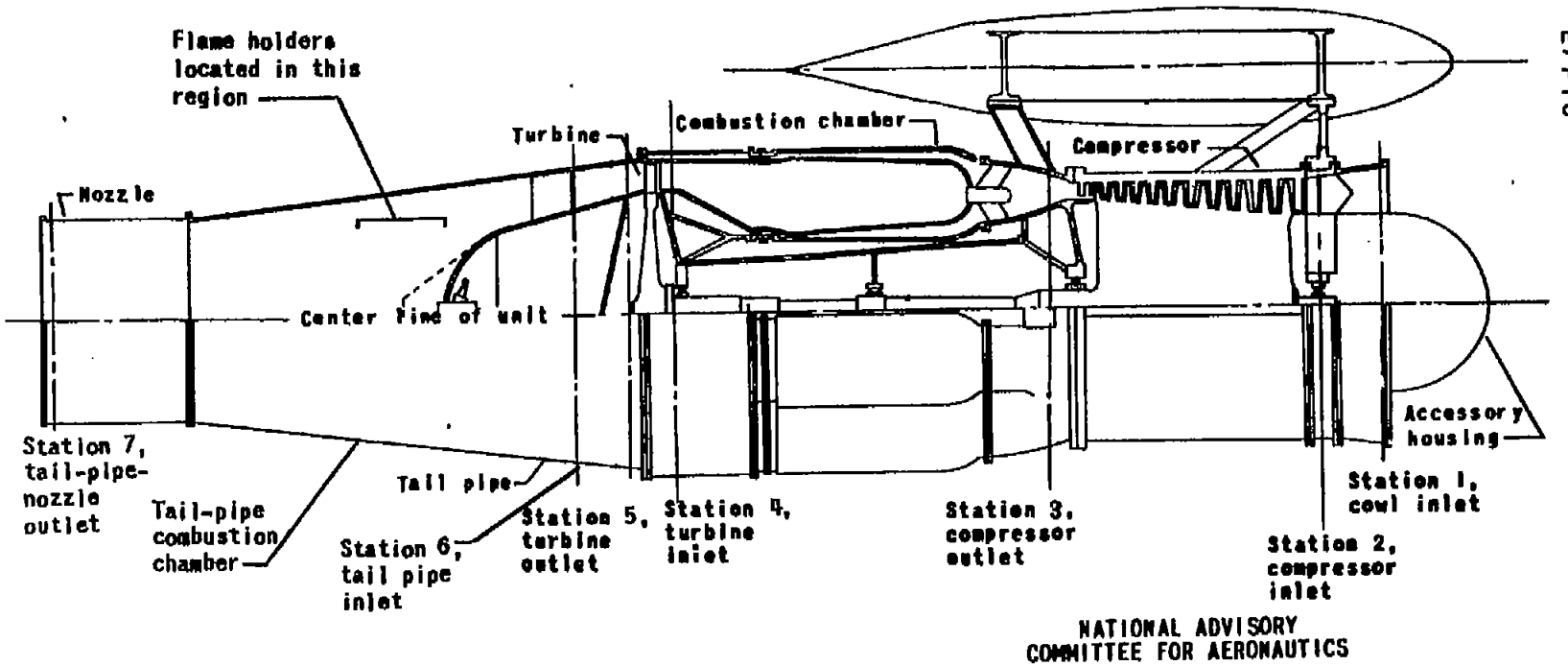

Figure 1. - Installation of standard turbojet engine with small tail-pipe combustion chamber showing relation of component parts and measuring stations in engine.

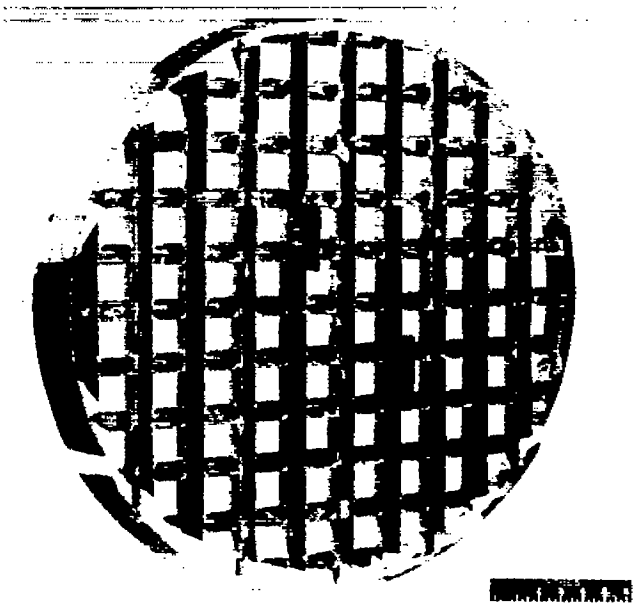

Figure 2. - Flame holder A composed of 30°-angle, V-type gutters spaced on $2\frac{1}{2}$-inch center lines; gutters 1 inch across open end.

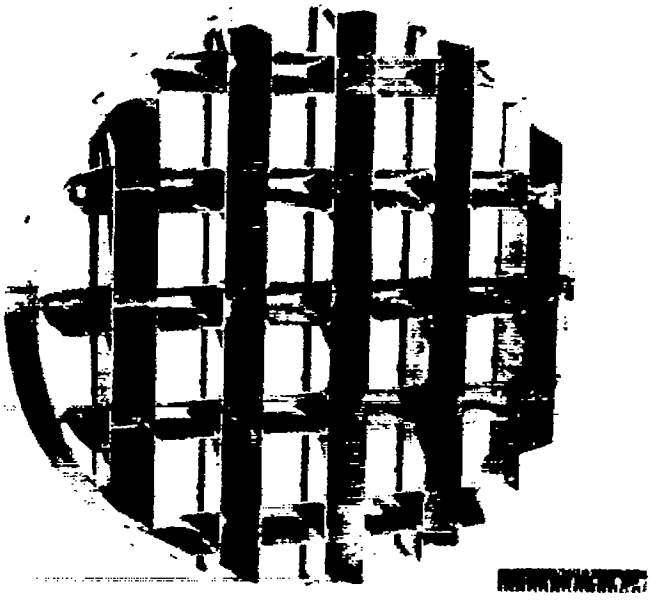

Figure 3. - Flame holder B composed of 30°-angle, V-type gutters spaced on 5-inch center lines; gutters 2 inches across open end.

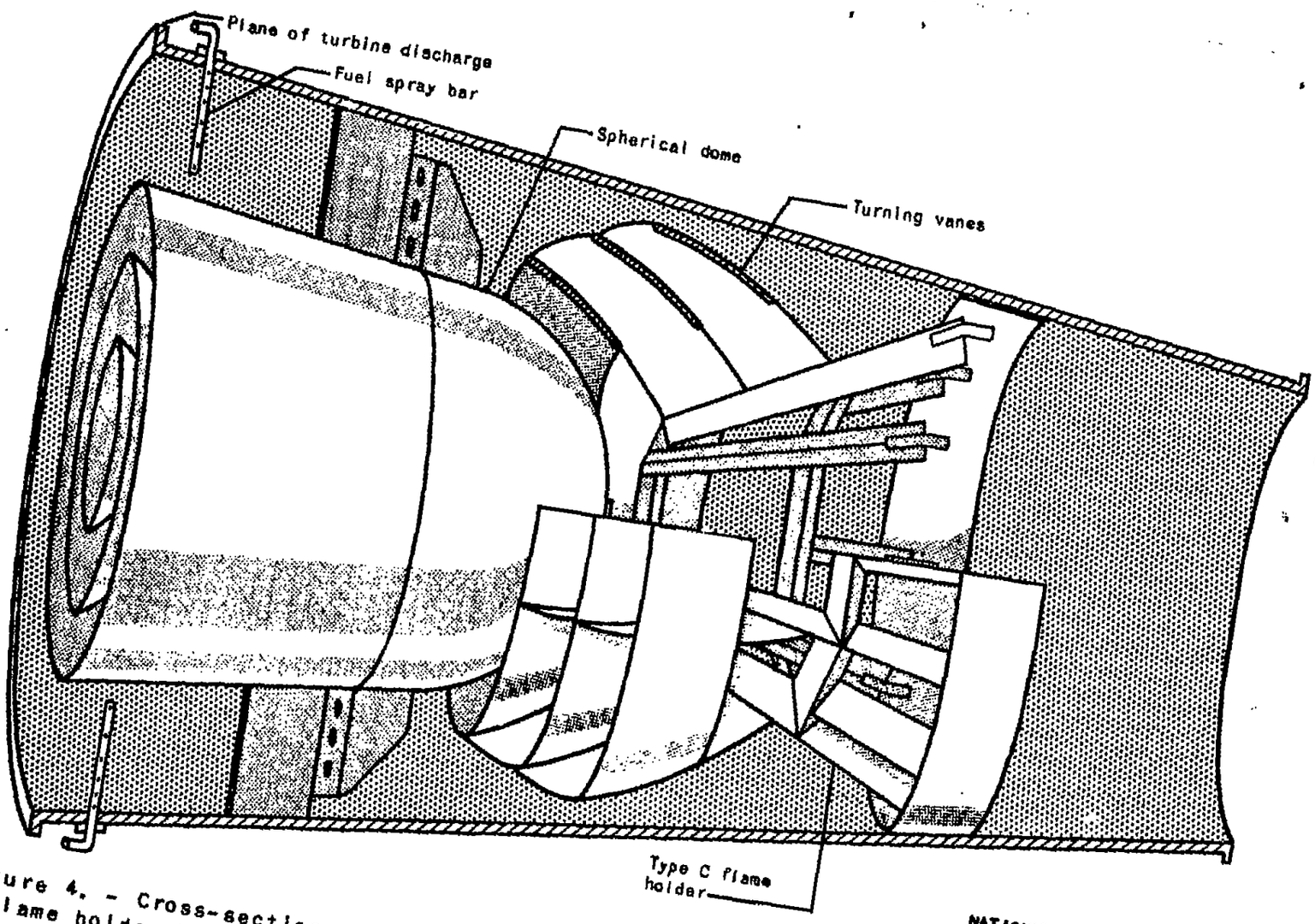

Figure 4. - Cross-section view of small tail-pipe combustion chamber showing type C flame holder having conical grid and circumferential turning vanes, fuel spray bars, and spherical dome on revised inner cone.

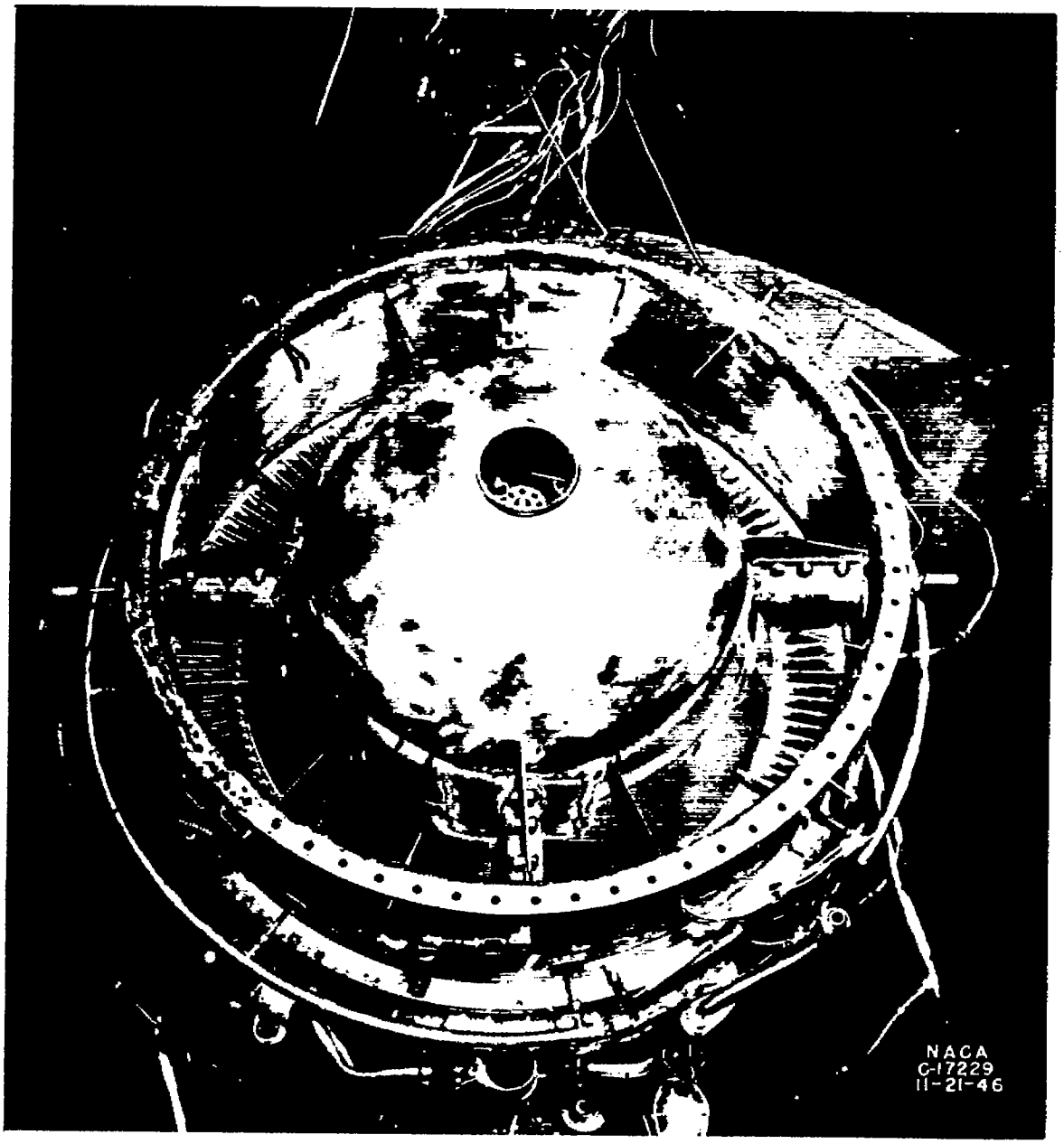

Figure 5. - Installation of spherical dome and ignition pilot in small tail-pipe combustion chamber.

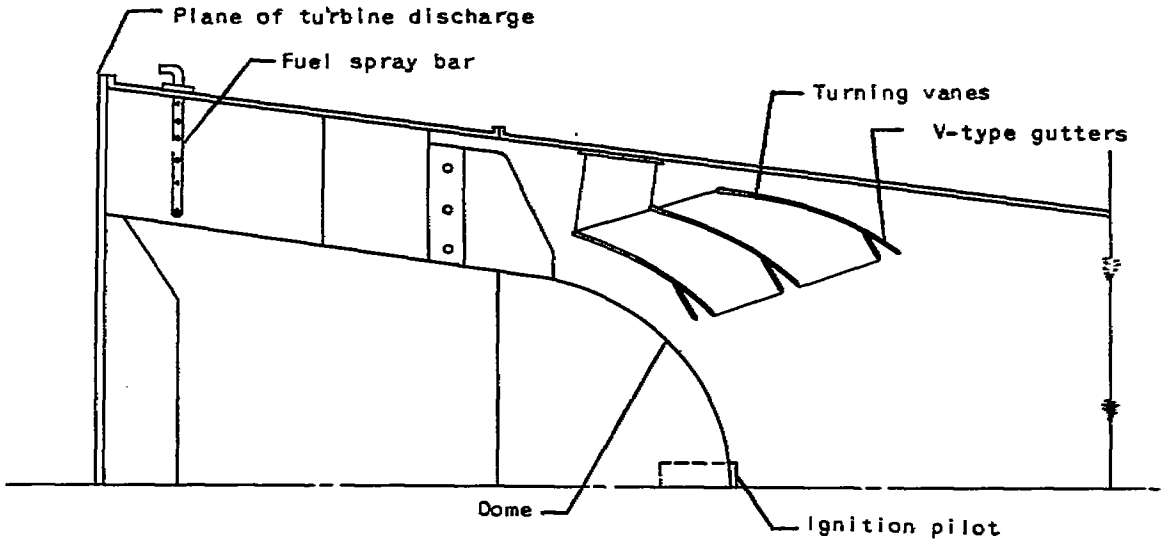

Figure 6. - Installation of type E turning-vane flame holder with 15°-angle, V-type gutters at trailing edge in small tail-pipe combustion chamber; gutters $\frac{3}{4}$ inch across open end.

NATIONAL ADVISORY
COMMITTEE FOR AERONAUTICS

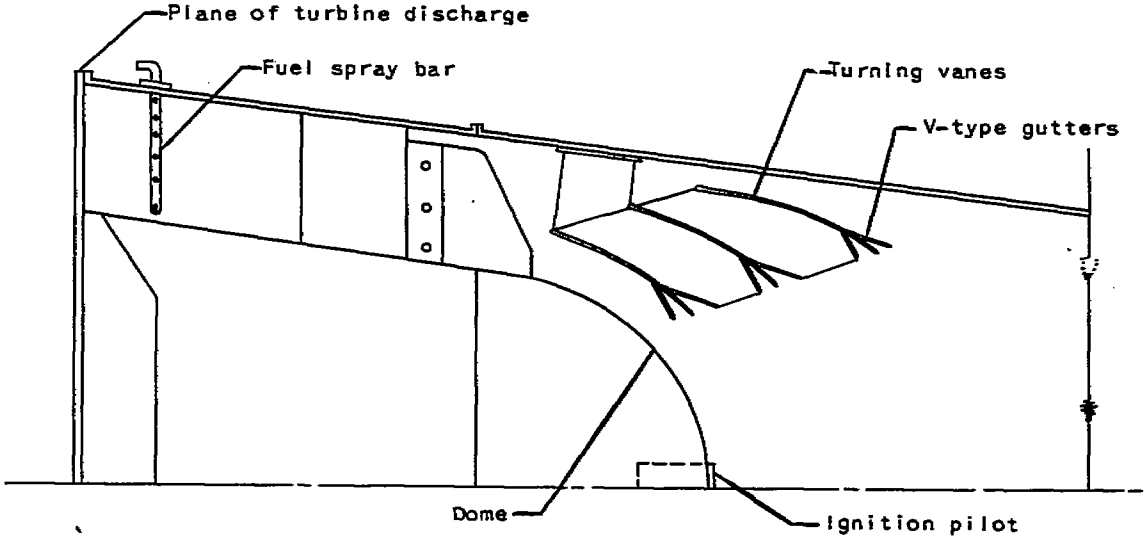

Figure 7. - Installation of type F turning-vane flame holder with 30°-angle, V-type gutters at trailing edge in small tail-pipe combustion chamber; gutters $1\frac{1}{2}$ inches across open end.

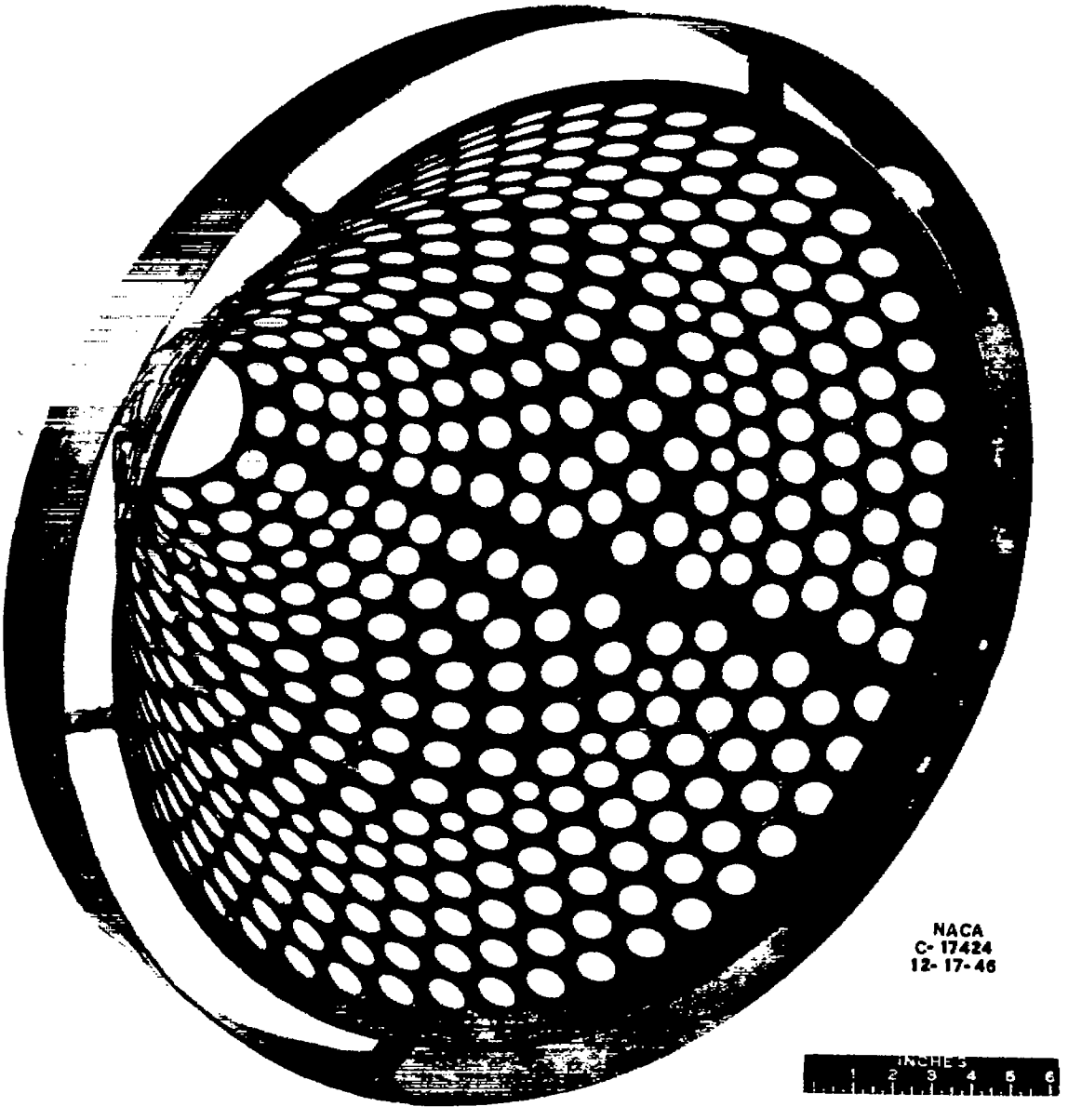

Figure 8. - Perforated conical flame holder G; diameter at upstream end, $26\frac{1}{2}$ inches; diameter at downstream end, $4\frac{1}{8}$ inches; length, 19 inches.

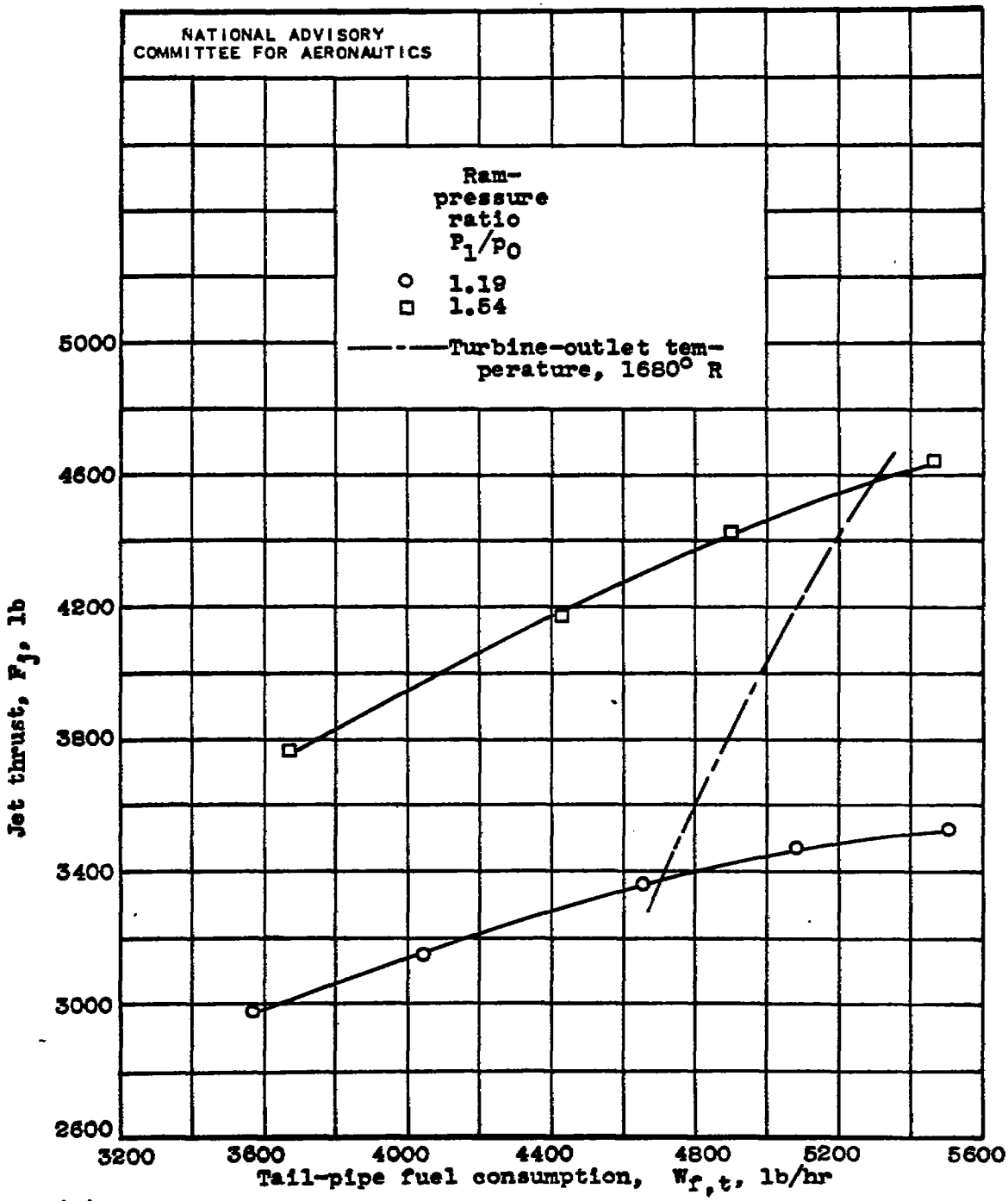

(a) Jet thrust.

Figure 9.- Variation of turbojet engine performance with tail-pipe fuel consumption for two ram-pressure ratios. Flame holder F; altitude, 20,000 feet; 21-inch-diameter tail-pipe nozzle.

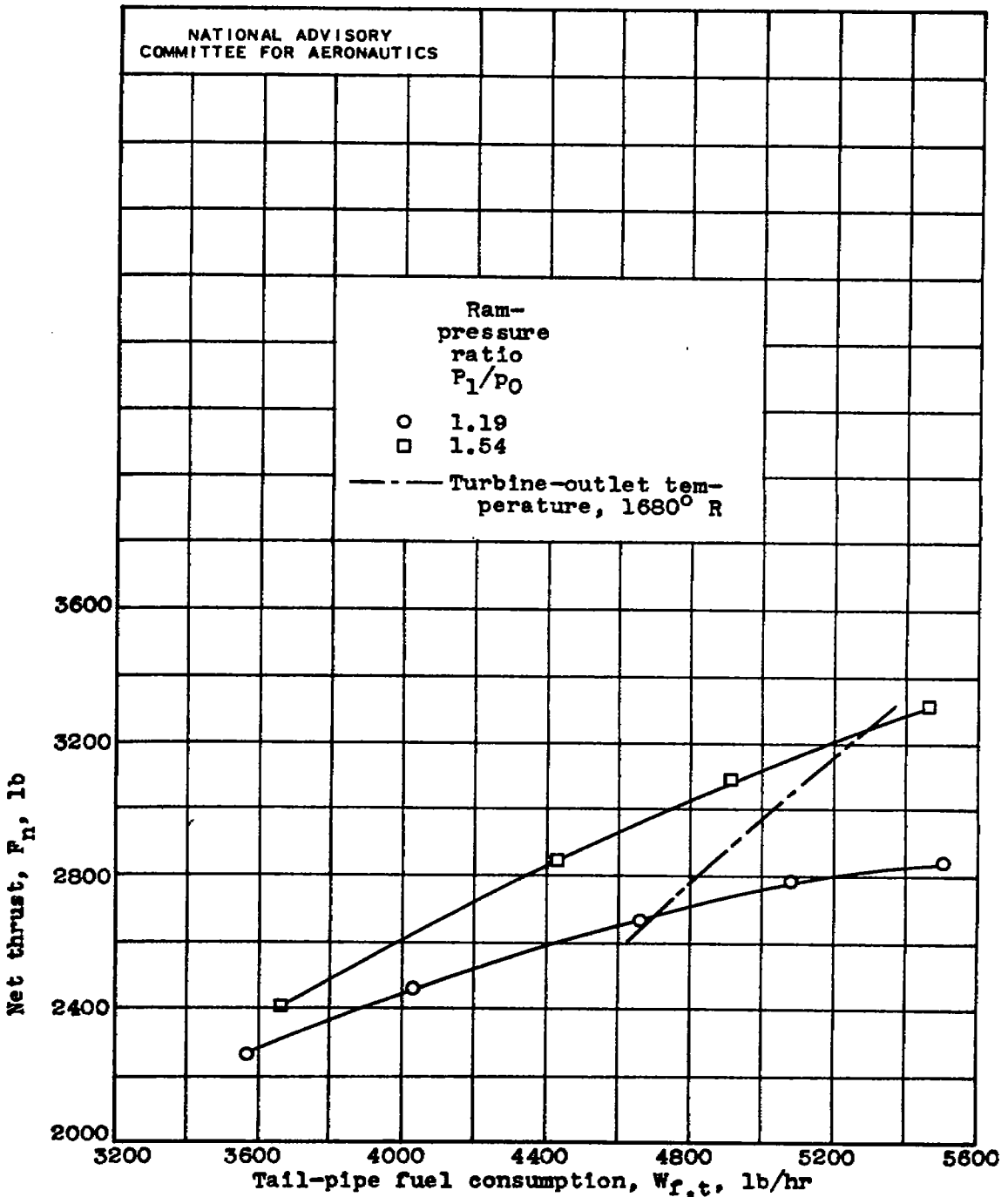

(b) Net thrust.

Figure 9.- Continued. Variation of turbojet engine performance with tail-pipe fuel consumption for two ram-pressure ratios. Flame holder F; altitude, 20,000 feet; 21-inch-diameter tail-pipe nozzle.

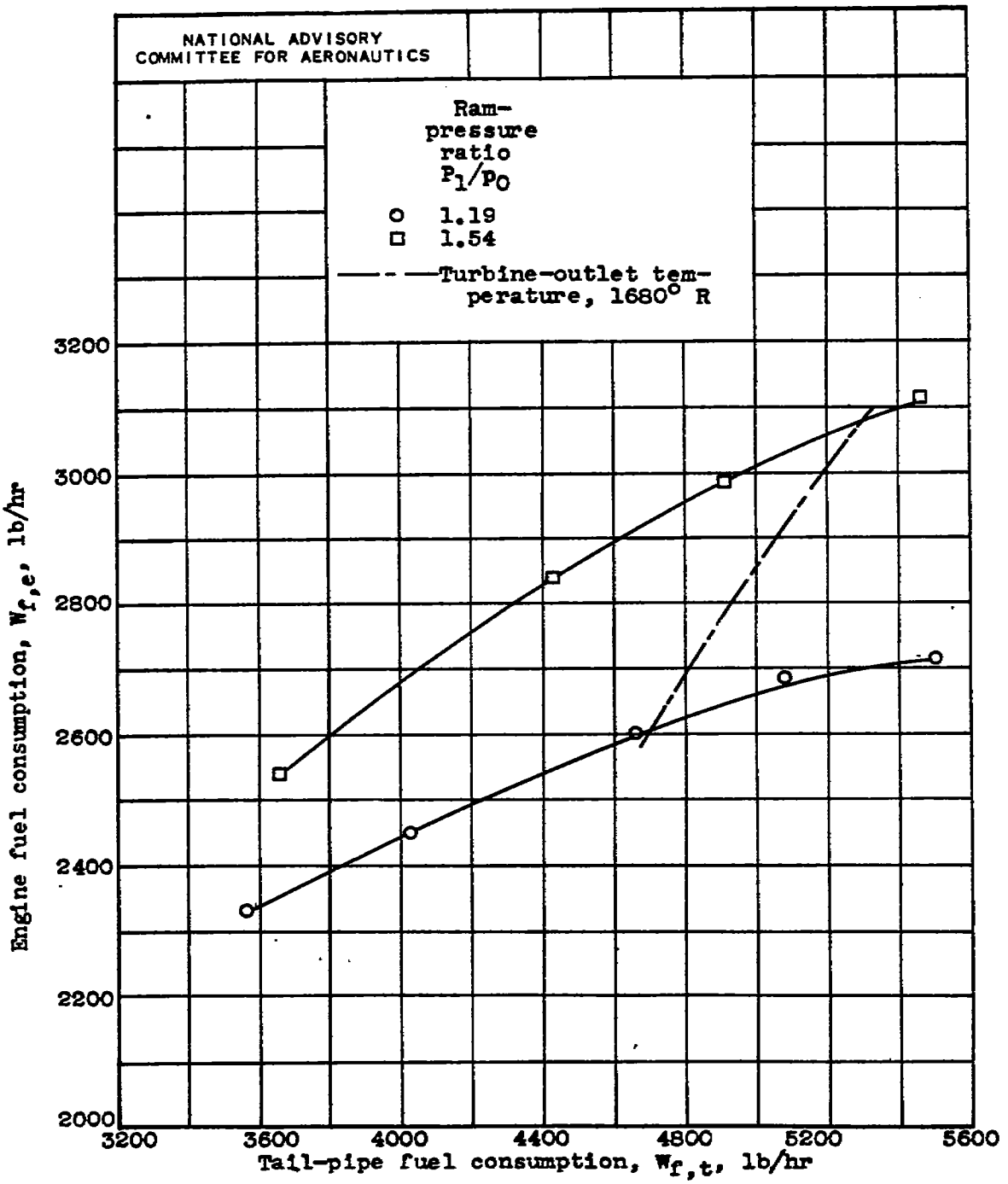

(c) Engine fuel consumption.

Figure 9.- Continued. Variation of turbojet engine performance with tail-pipe fuel consumption for two ram-pressure ratios. Flame holder F; altitude, 20,000 feet; 21-inch-diameter tail-pipe nozzle.

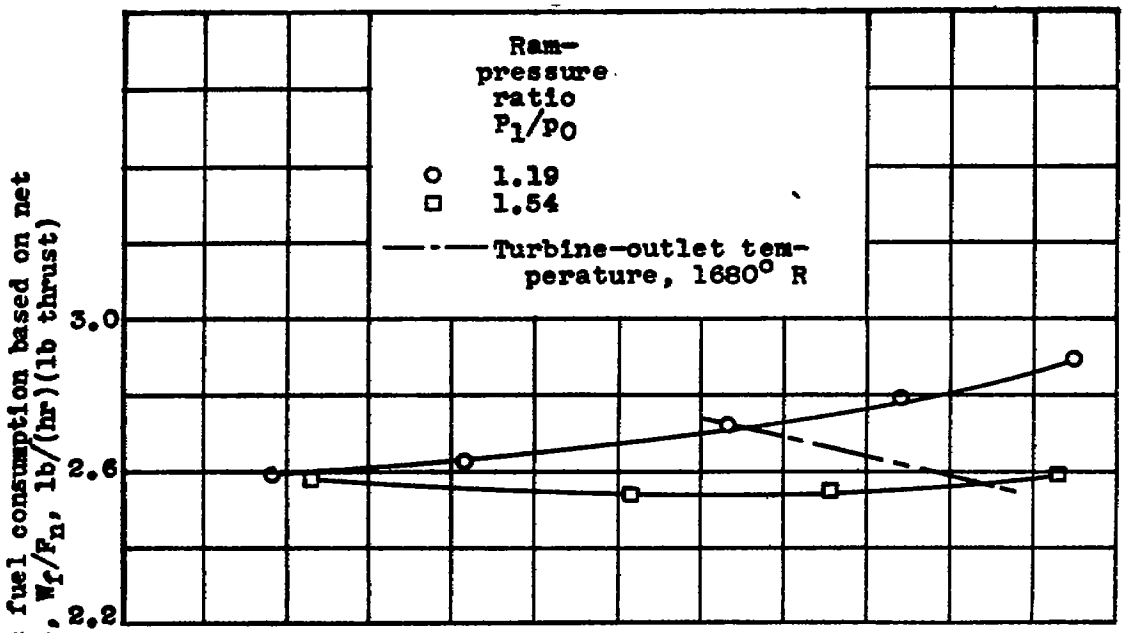

(d) Specific fuel consumption based on net thrust.

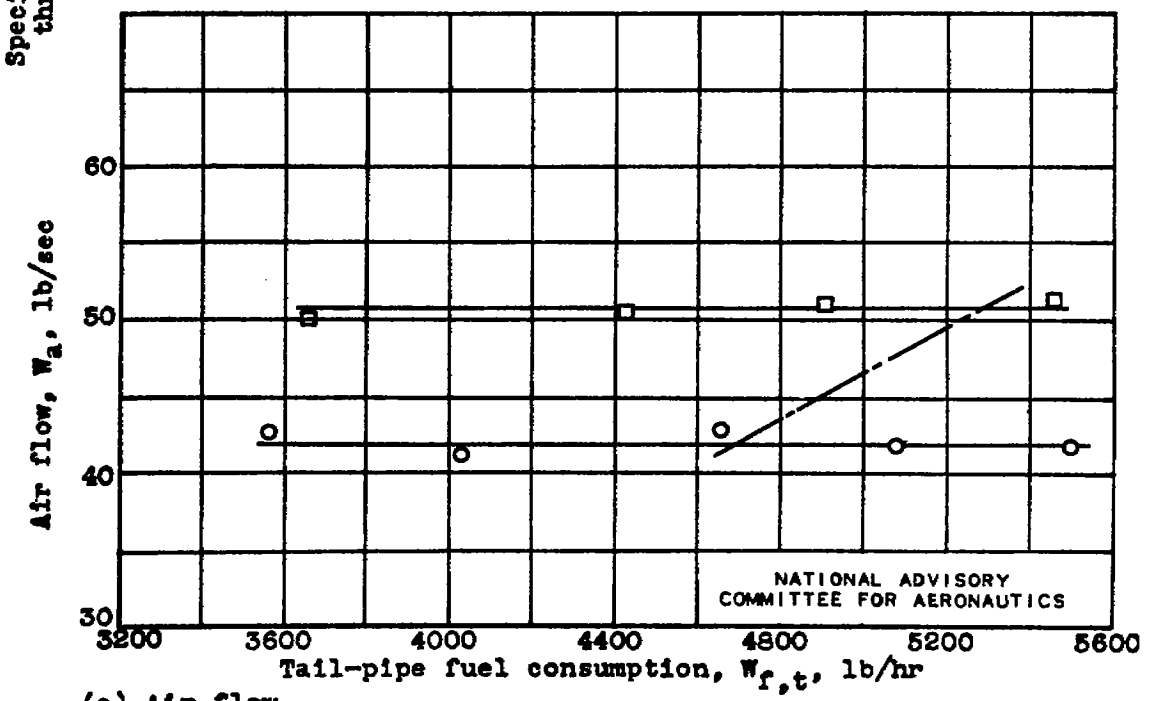

(e) Air flow.

Figure 9.- Continued. Variation of turbojet engine performance with tail-pipe fuel consumption for two ram-pressure ratios. Flame holder F; altitude, 20,000 feet; 21-inch-diameter tail-pipe nozzle.

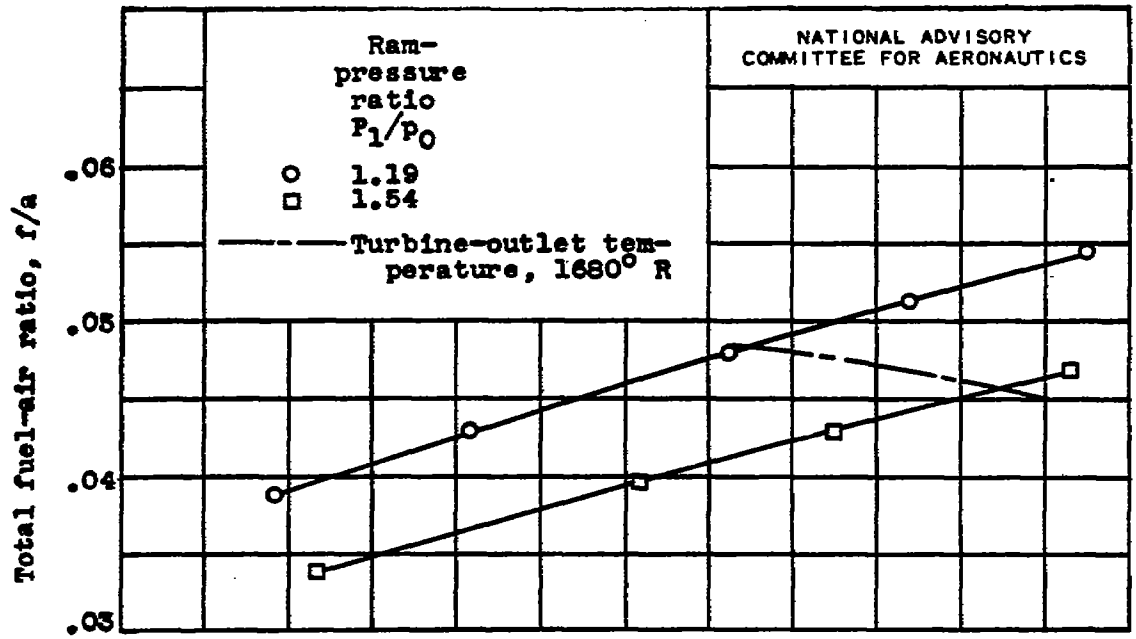

(f) Total fuel-air ratio.

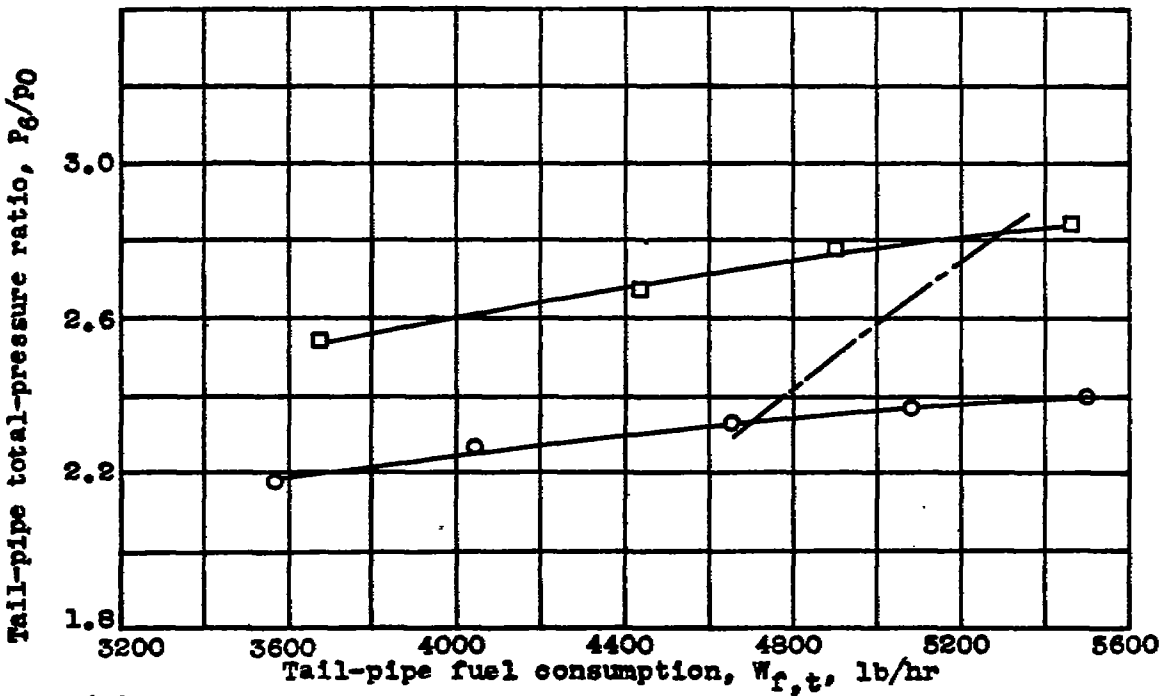

(g) Tail-pipe total-pressure ratio.

Figure 9.- Concluded. Variation of turbojet engine performance with tail-pipe fuel consumption for two ram-pressure ratios. Flame holder F; altitude, 20,000 feet; 21-inch-diameter tail-pipe nozzle.

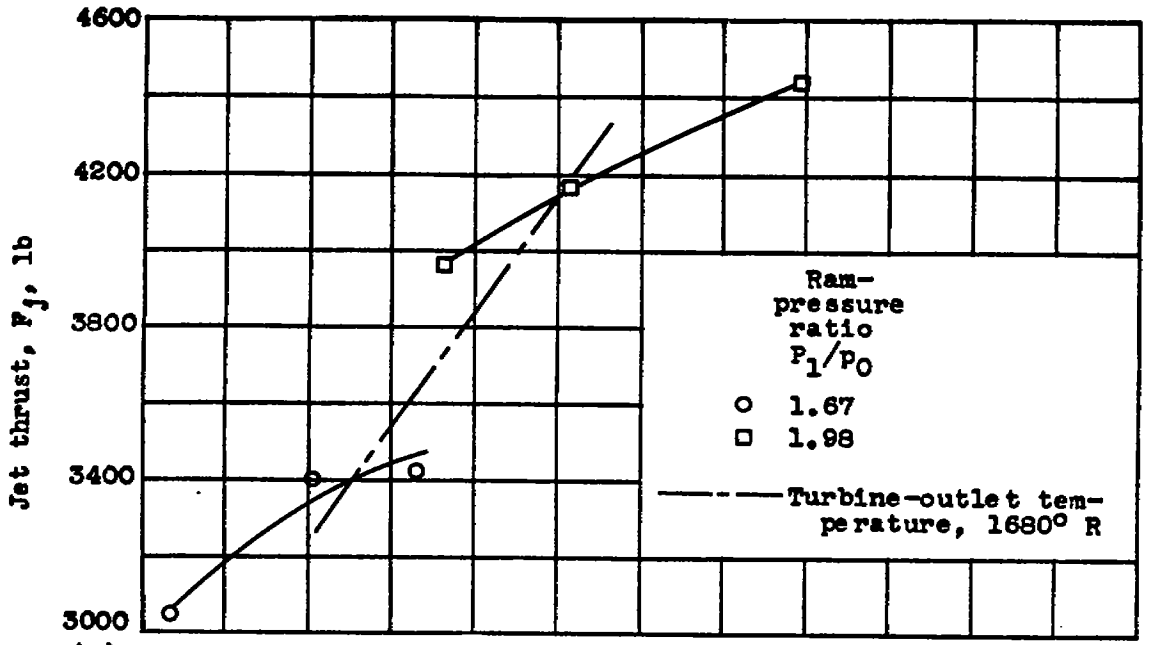

(a) Jet thrust.

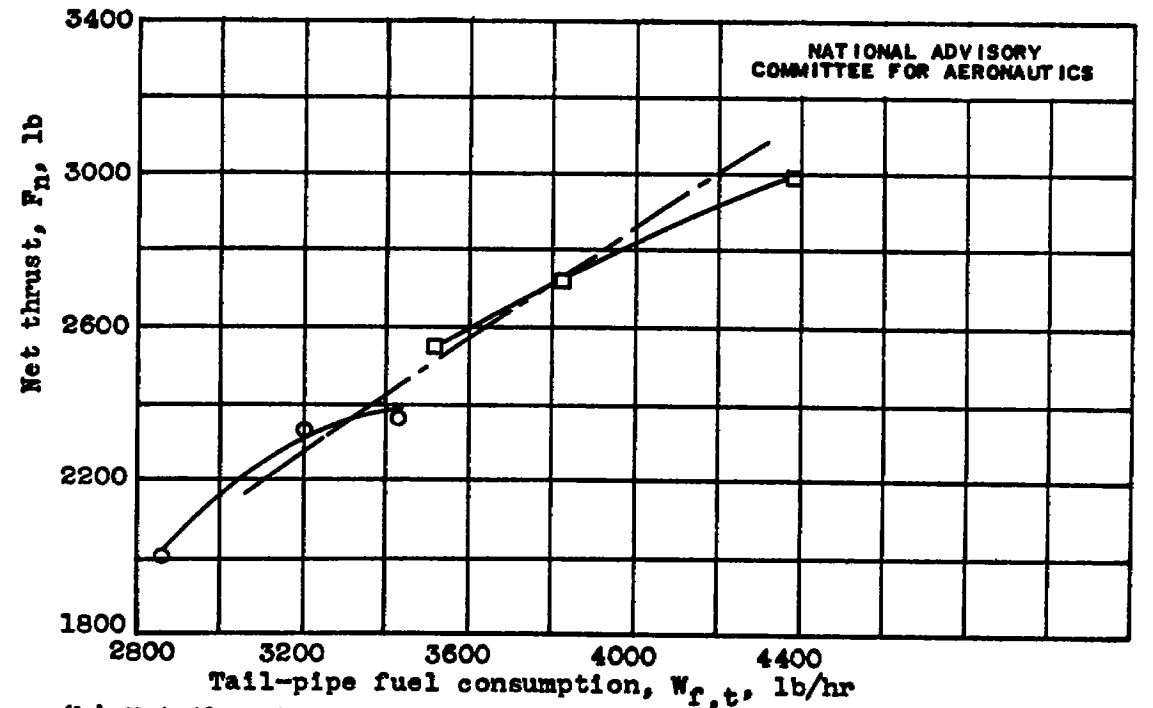

(b) Net thrust.

Figure 10.- Variation of turbojet engine performance with tail-pipe fuel consumption for two ram-pressure ratios. Flame holder C; altitude, 30,000 feet; 21-inch-diameter tail-pipe nozzle.

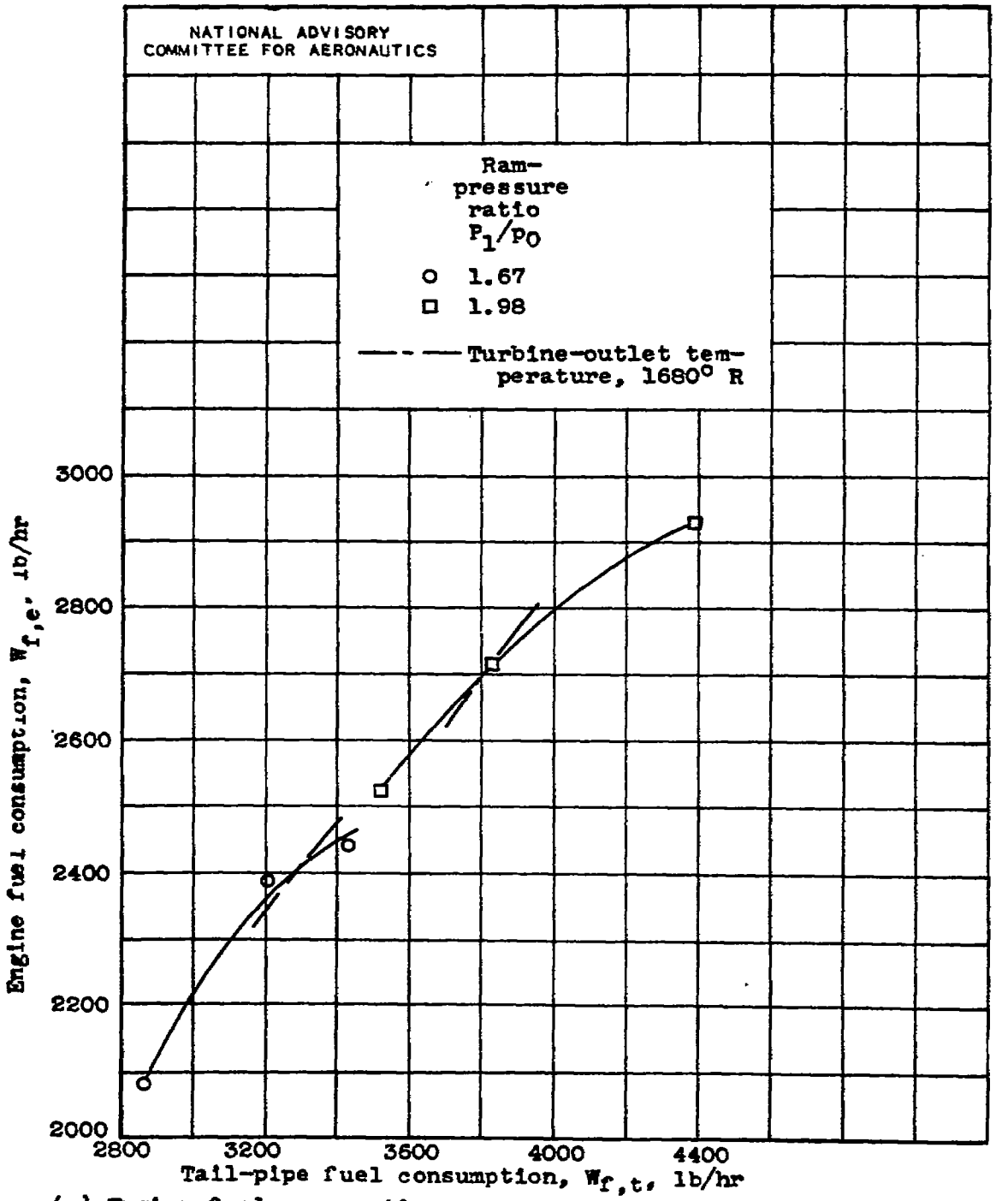

(c) Engine fuel consumption.

Figure 10.- Continued. Variation of turbojet engine performance with tail-pipe fuel consumption for two ram-pressure ratios. Flame holder C; altitude, 30,000 feet; 21-inch-diameter tail-pipe nozzle.

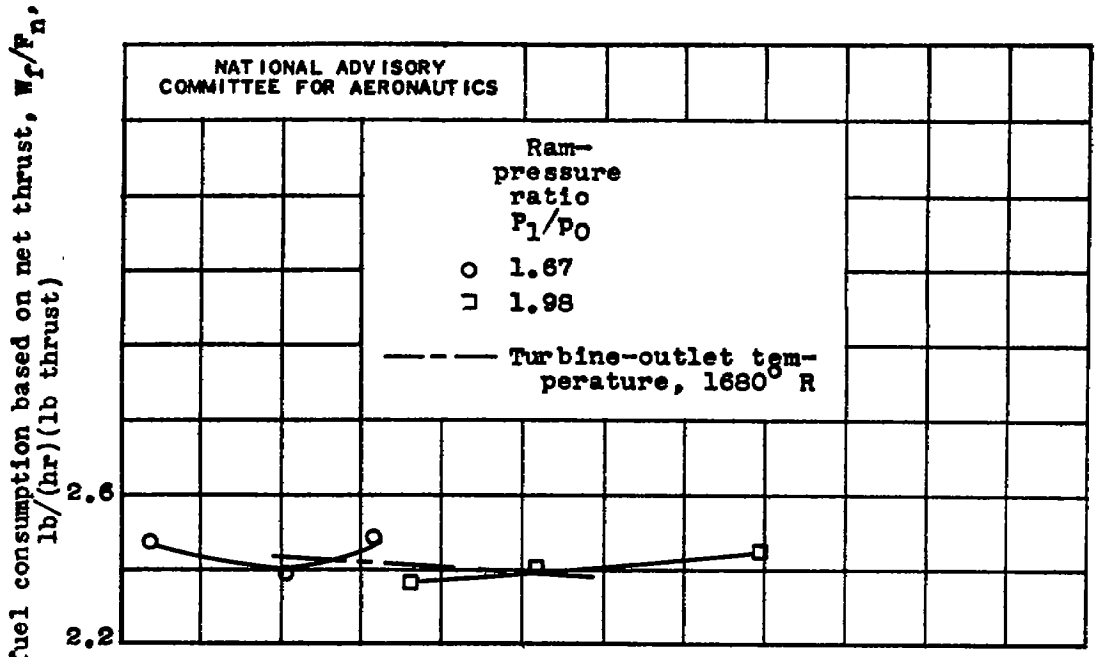

(d) Specific fuel consumption based on net thrust.

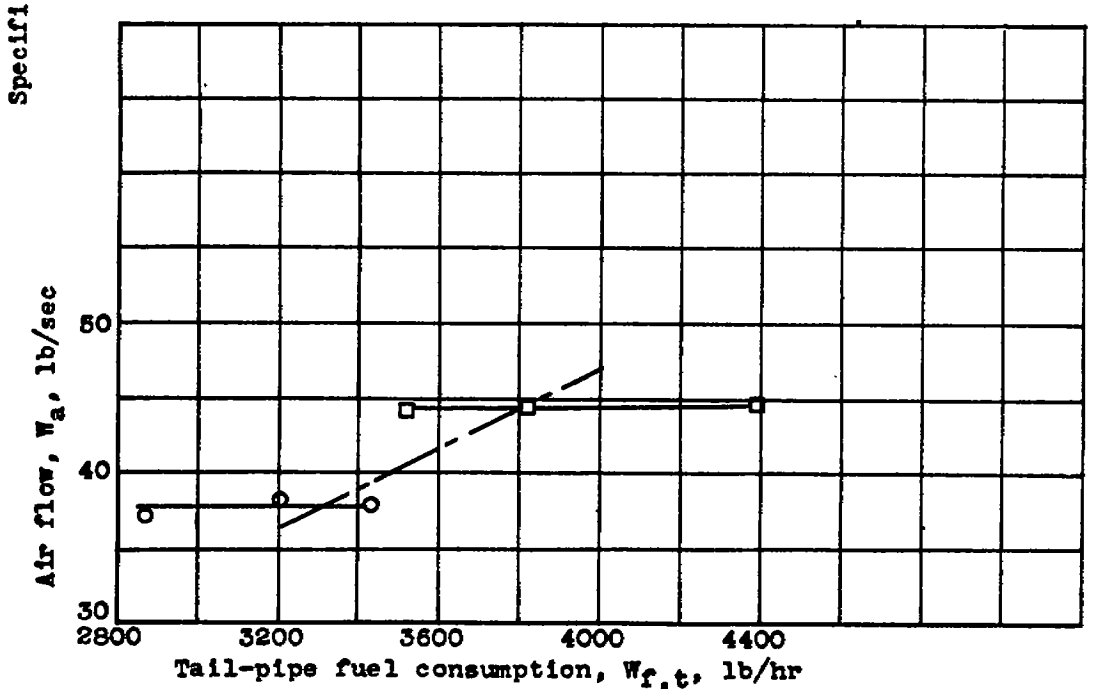

(e) Air flow.

Figure 10.- Continued. Variation of turbojet engine performance with tail-pipe fuel consumption for two ram-pressure ratios. Flame holder C; altitude, 30,000 feet; 21-inch-diameter tail-pipe nozzle.

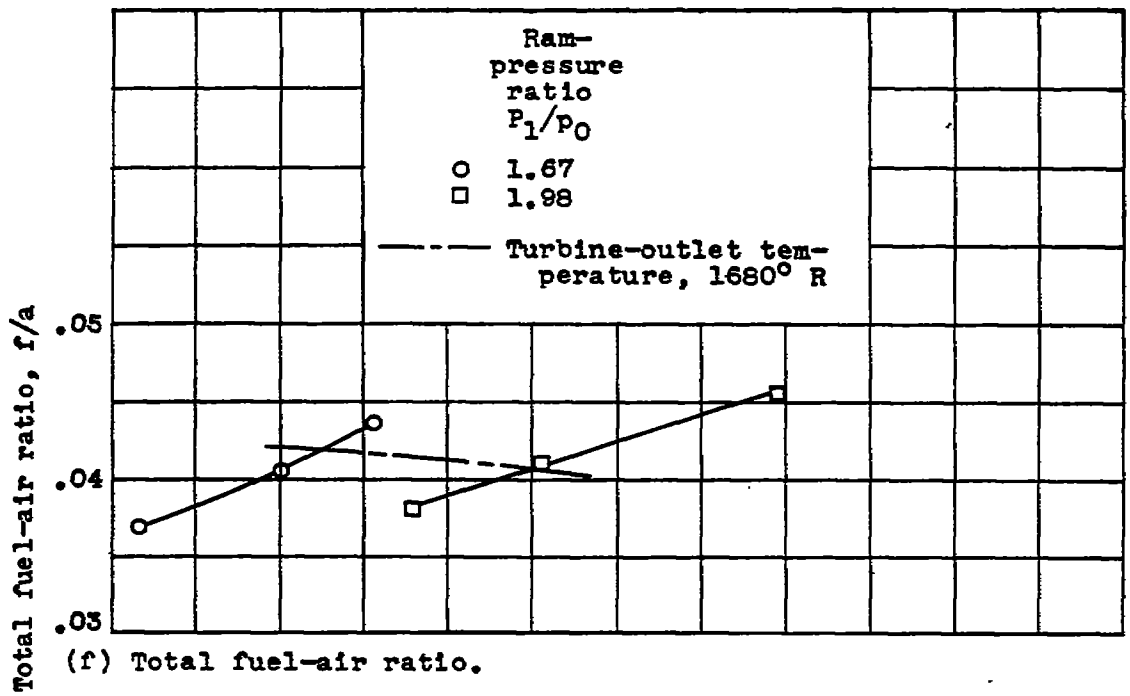

(f) Total fuel-air ratio.

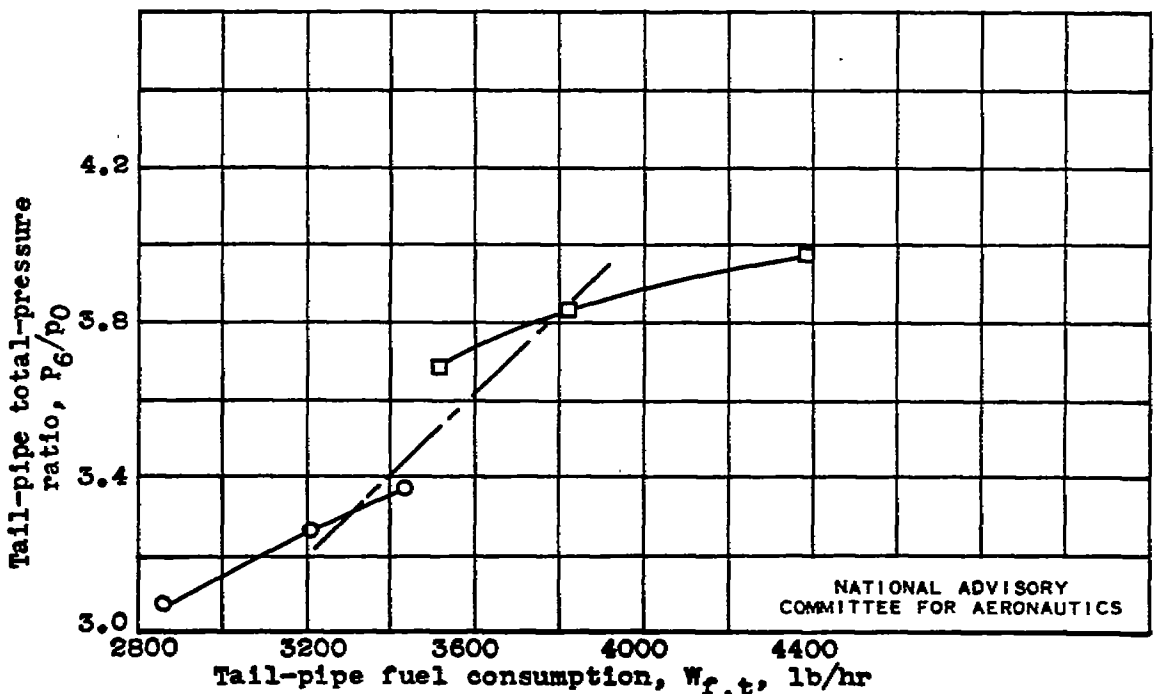

(g) Tail-pipe total pressure ratio.

Figure 10.- Concluded. Variation of turbojet engine performance with tail-pipe fuel consumption for two ram-pressure ratios. Flame holder C; altitude, 30,000 feet; 21-inch-diameter tail-pipe nozzle.

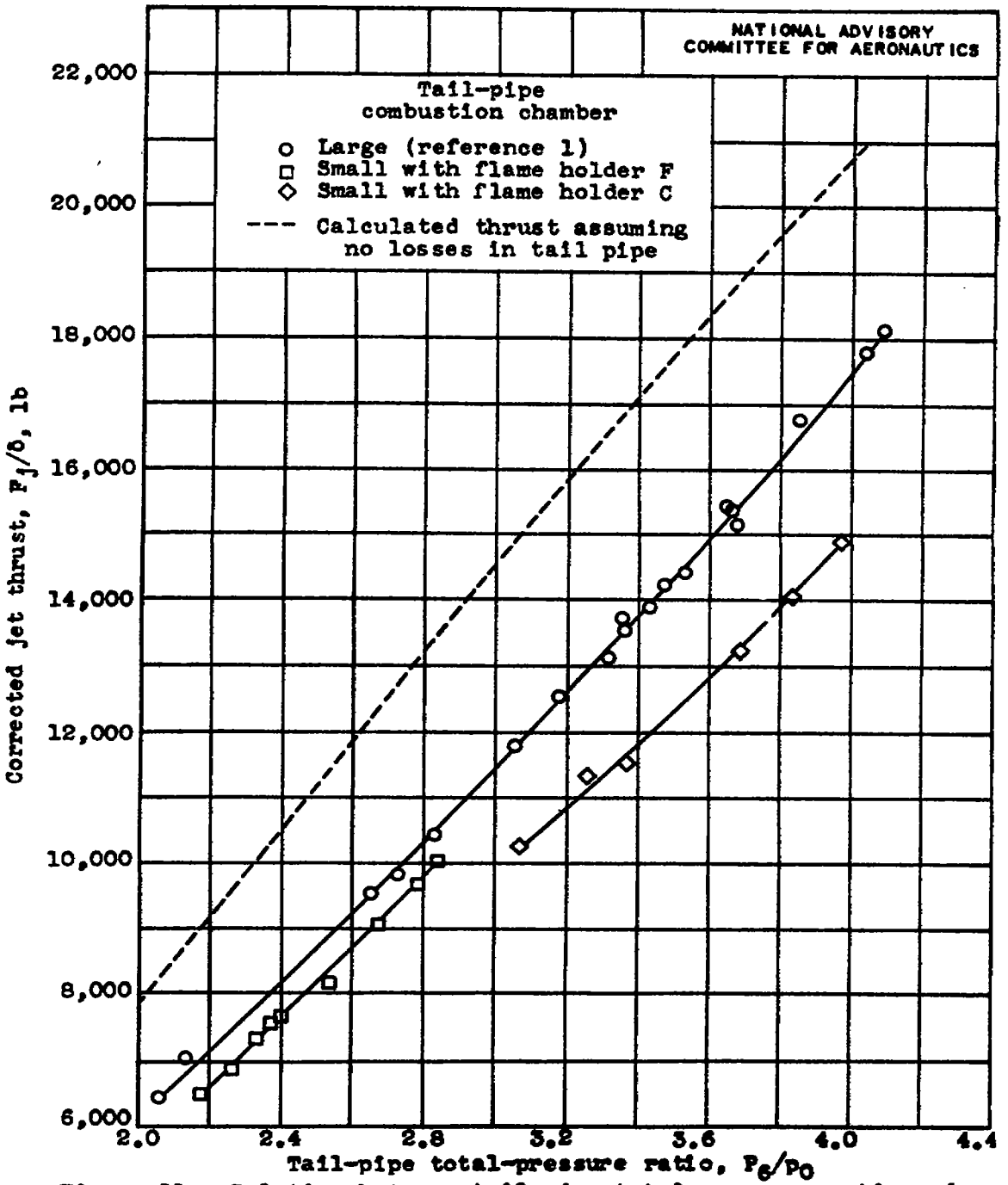

Figure 11.- Relation between tail-pipe total-pressure ratio and corrected jet thrust of turbojet engine with large tail-pipe combustion chamber (reference 1) and small tail pipe with flame holders C and F. Engine speed, 7600 rpm; 21-inch-diameter tail-pipe nozzle.

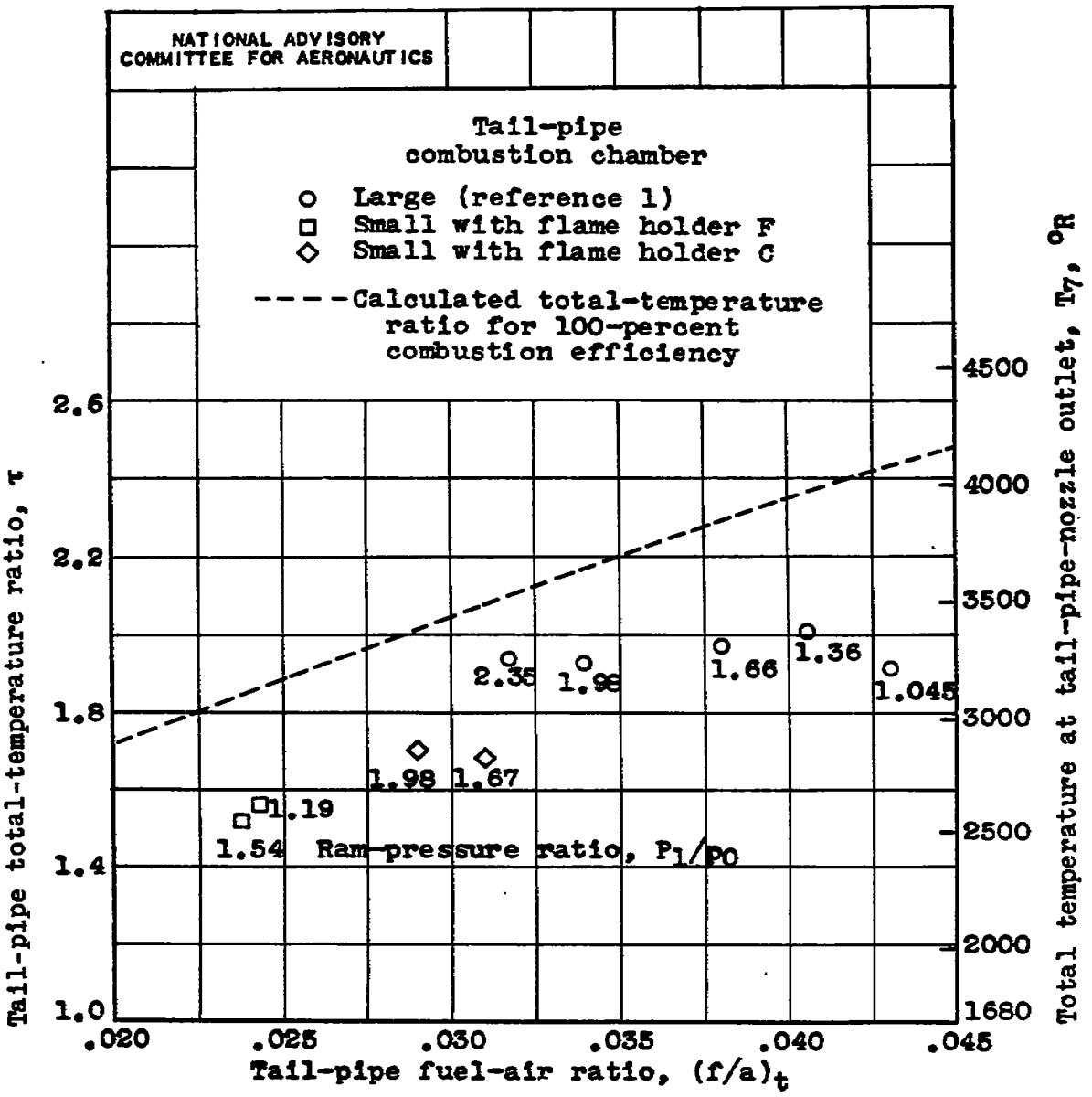

Figure 12.- Relation among tail-pipe total-temperature ratio, tail-pipe-nozzle-outlet total temperature, and tail-pipe fuel-air ratio of turbojet engine with large tail pipe combustion chamber (reference 1) and small tail pipe with flame holders C and F. Engine speed, 7600 rpm; 21-inch-diameter tail-pipe nozzle; turbine-outlet temperature, 1680° R.

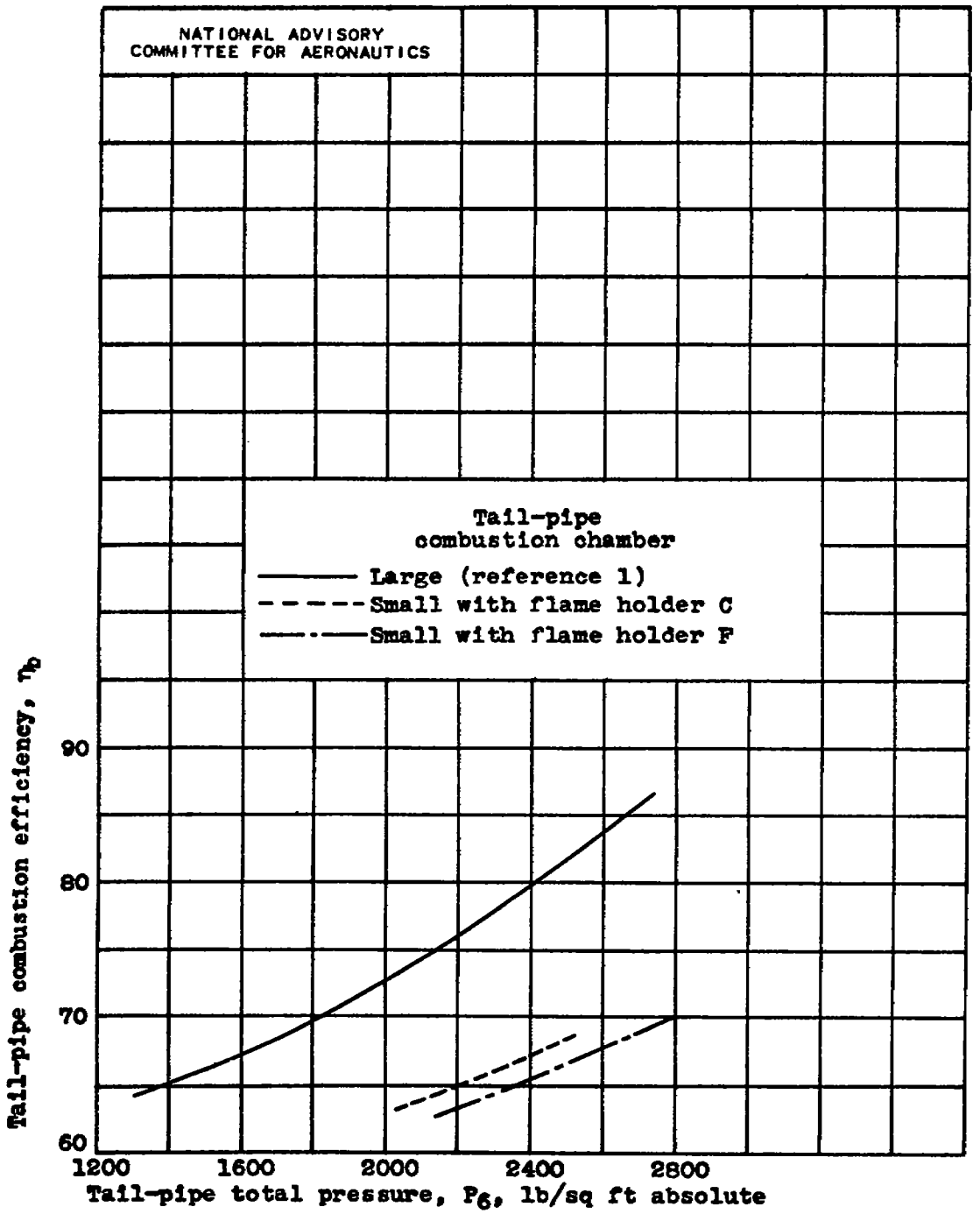

Figure 13.- Relation between tail-pipe combustion efficiency and tail-pipe total pressure of turbojet engine with large tail-pipe combustion chamber (reference 1) and small tail pipe with two flame holders. Engine speed, 7600 rpm; turbine-outlet temperature, 1680° R; 21-inch-diameter tail-pipe nozzle.

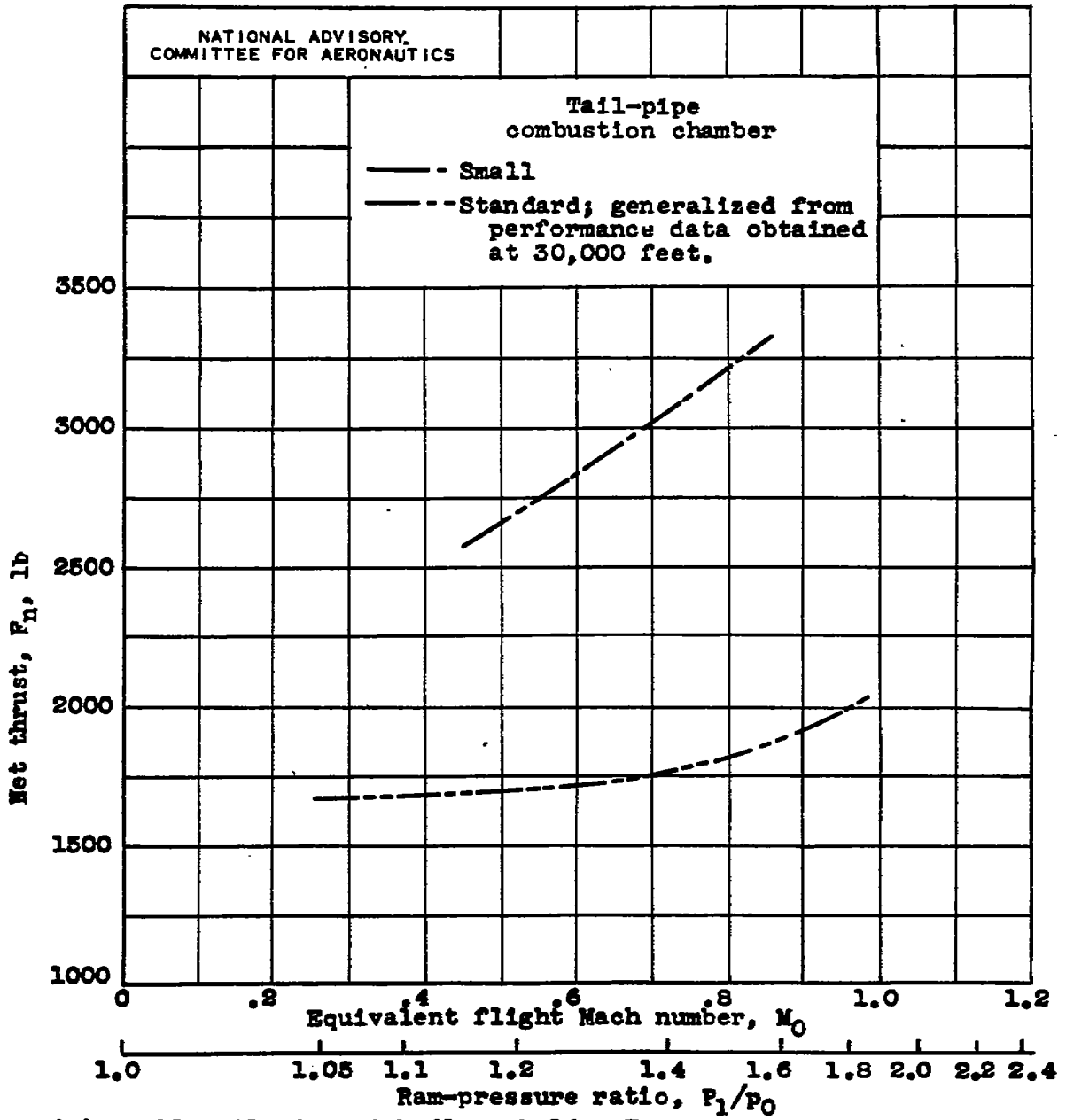

(a) Small tail pipe with flame holder F. Pressure altitude, 20,000 feet.

Figure 14.- Relation between equivalent flight Mach number and net thrust of turbojet engine with standard tail pipe and with tail-pipe burning in modified tail pipes. Engine speed, 7600 rpm; 21-inch-diameter tail-pipe nozzle with tail-pipe burning; turbine-outlet temperature with tail-pipe burning, 1680° R; $16\frac{3}{4}$-inch-diameter nozzle on standard tail pipe.

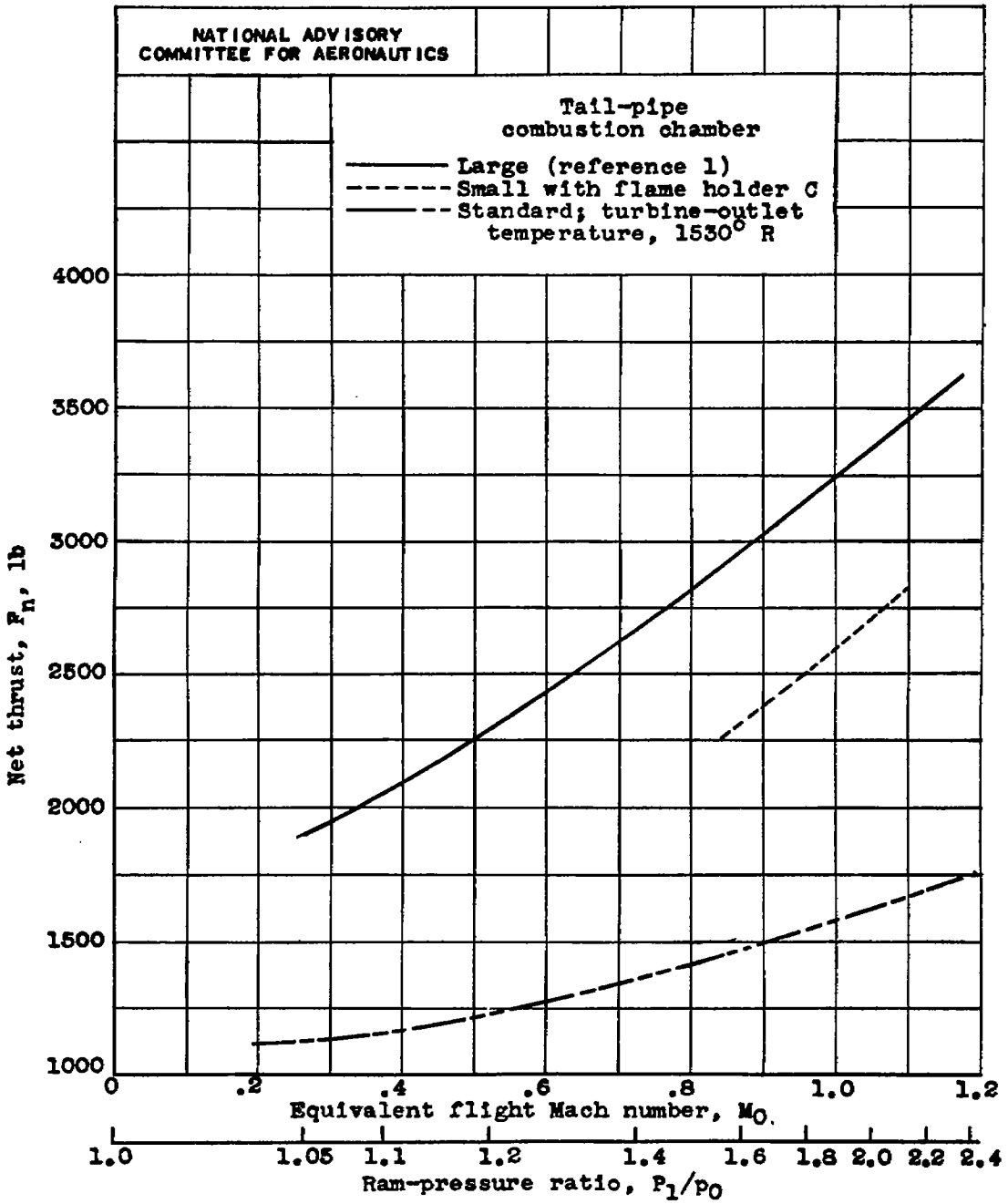

(b) Large tail-pipe combustion chamber (reference 1) and small tail pipe with flame holder C. Pressure altitude, 30,000 feet.

Figure 14.- Concluded. Relation between equivalent flight Mach number and net thrust of turbojet engine with standard tail pipe and with tail-pipe burning in modified tail pipes. Engine speed, 7600 rpm; 21-inch-diameter tail-pipe nozzle with tail-pipe burning; turbine-outlet temperature with tail-pipe burning, 1680° R; $16\frac{3}{4}$-inch-diameter nozzle on standard tail pipe.

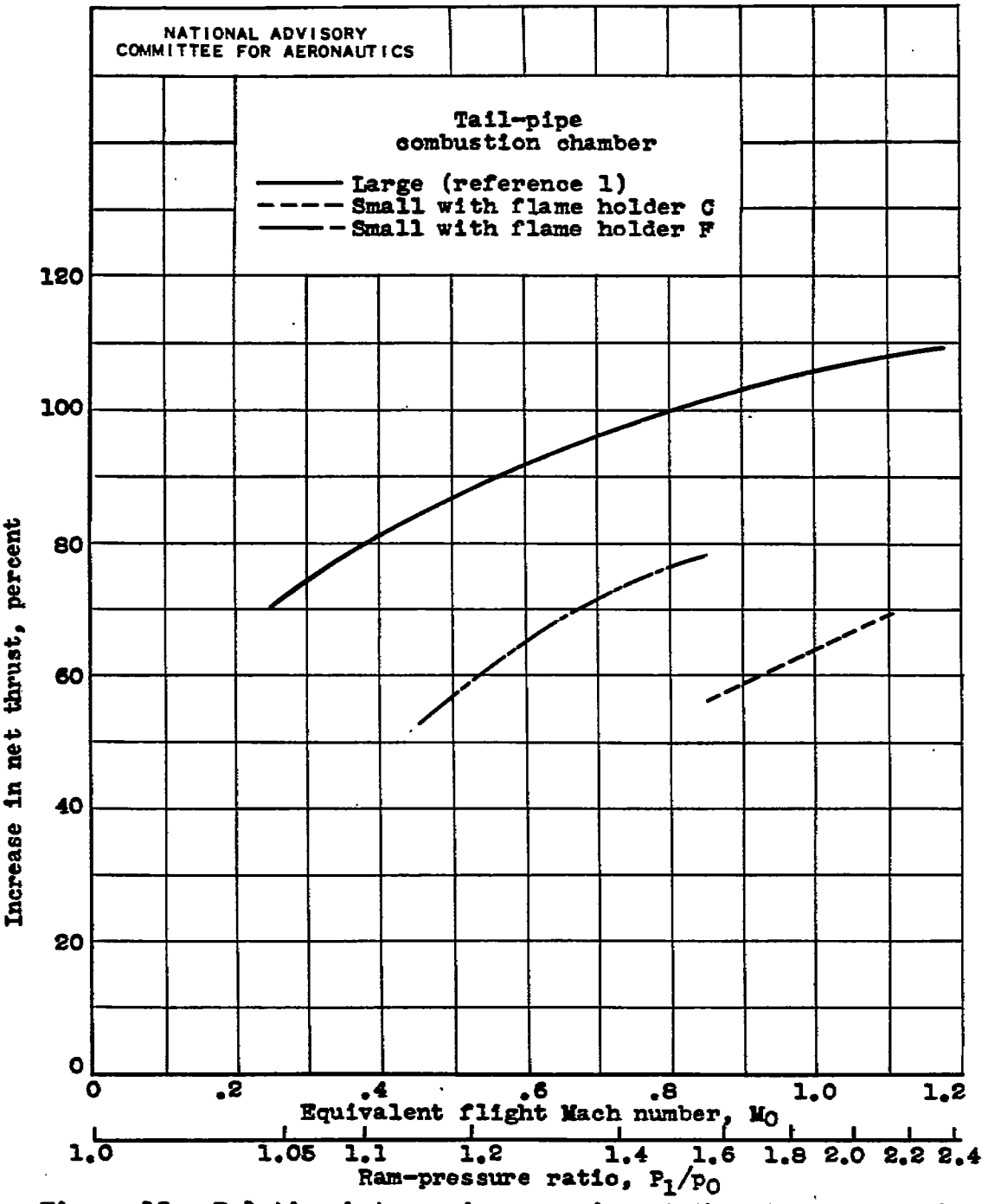

Figure 15.- Relation between increase in net thrust and equivalent flight Mach number of turbojet engine with large tail-pipe combustion chamber (reference 1) and small tail pipe with flame holders C and F. Engine speed, 7600 rpm; 21-inch-diameter tail-pipe nozzle; turbine-outlet temperature with tail-pipe burning, 1680° R.

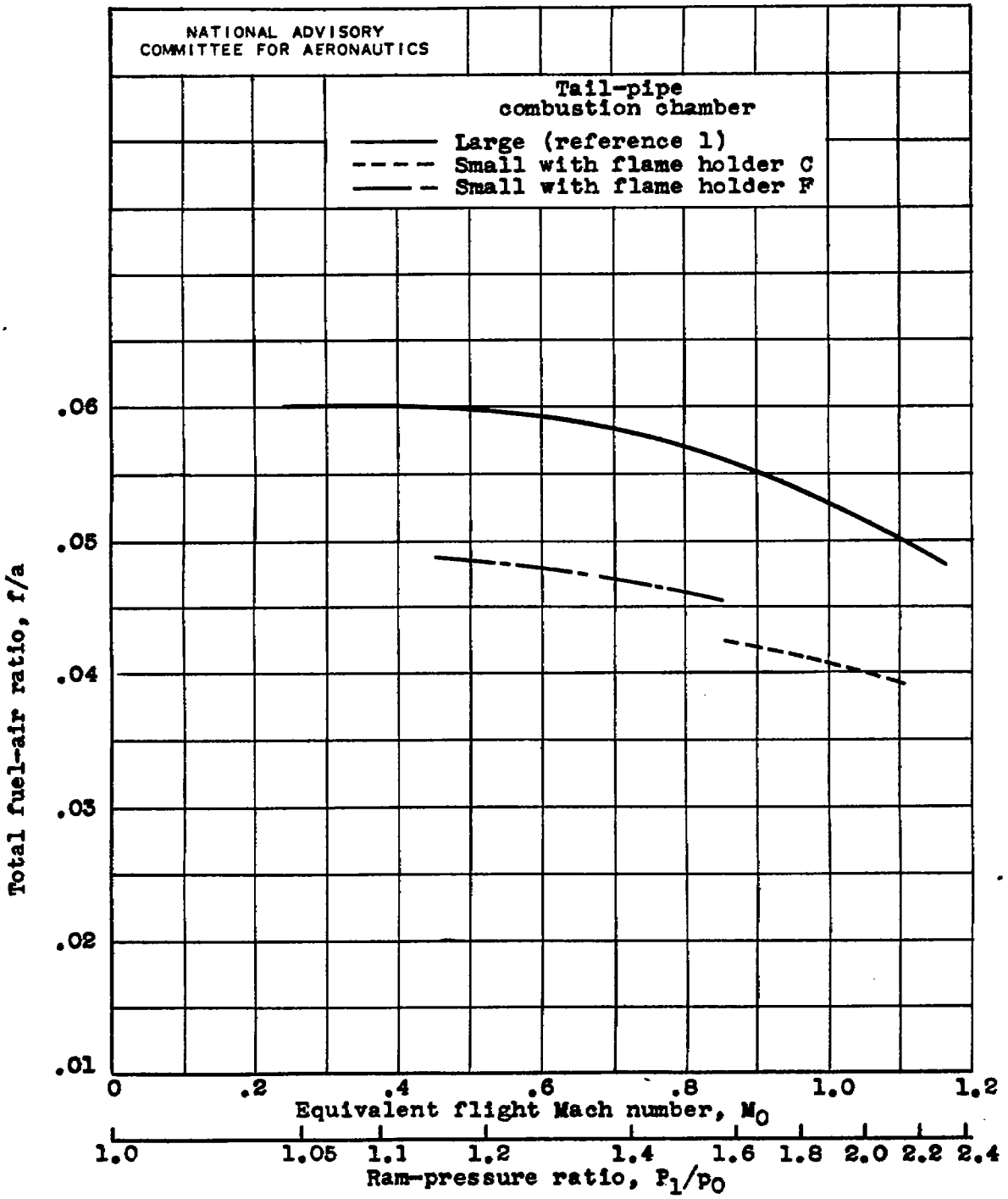

Figure 16.- Relation between total fuel-air ratio and equivalent flight Mach number of turbojet engine with large tail-pipe combustion chamber (reference 1) and small tail pipe with flame holders C and F. Engine speed, 7600 rpm; 21-inch-diameter tail-pipe nozzle; turbine-outlet temperature, 1680° R.

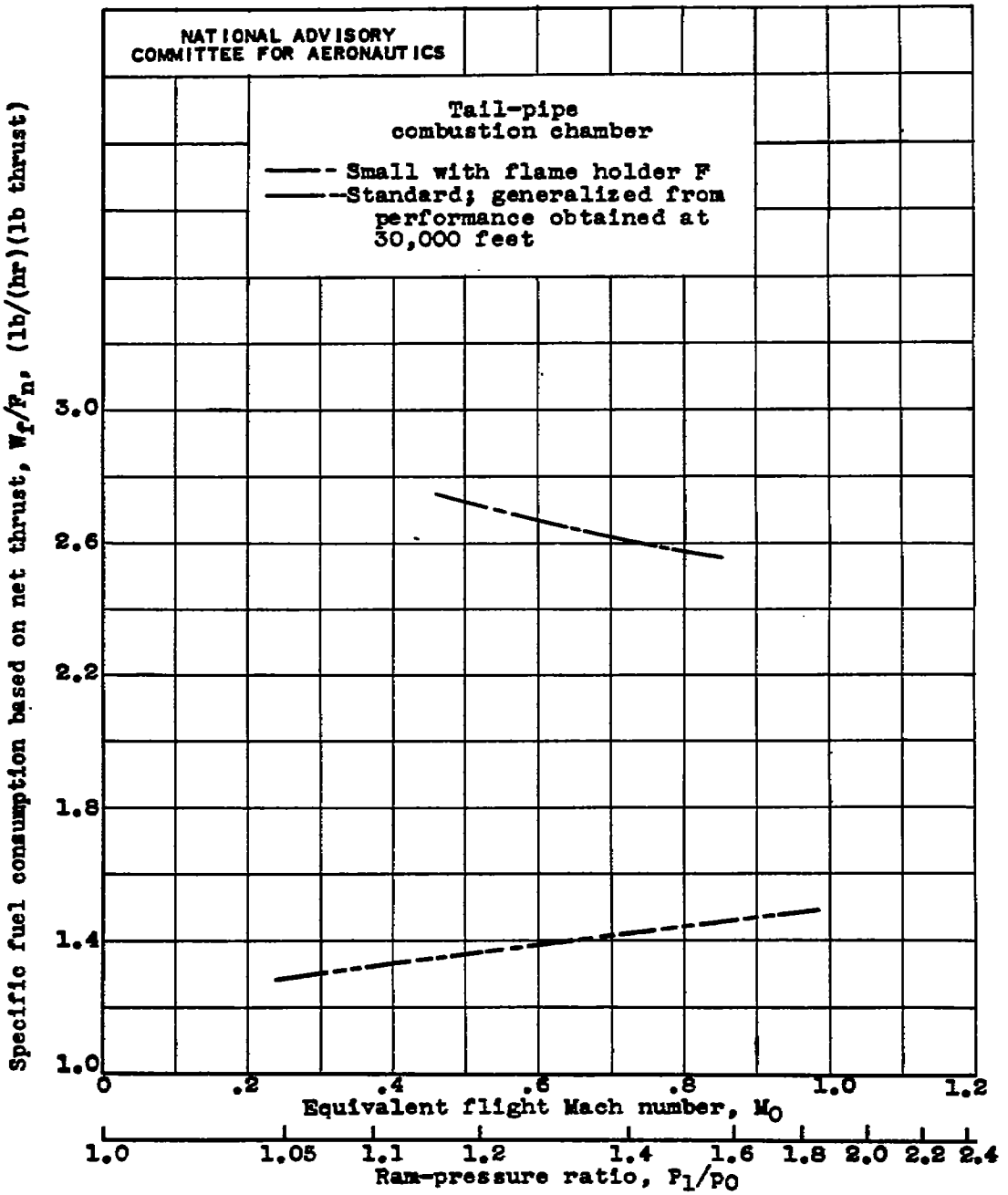

(a) Small tail pipe with flame holder F. Pressure altitude, 20,000 feet.

Figure 17.- Relation between specific fuel consumption based on net thrust and equivalent flight Mach number of turbojet engine with standard tail pipe and with tail-pipe burning in modified tail pipes. Engine speed, 7600 rpm; 21-inch-diameter tail-pipe nozzle with tail-pipe burning; turbine-outlet temperature with tail-pipe burning, 1680° R.

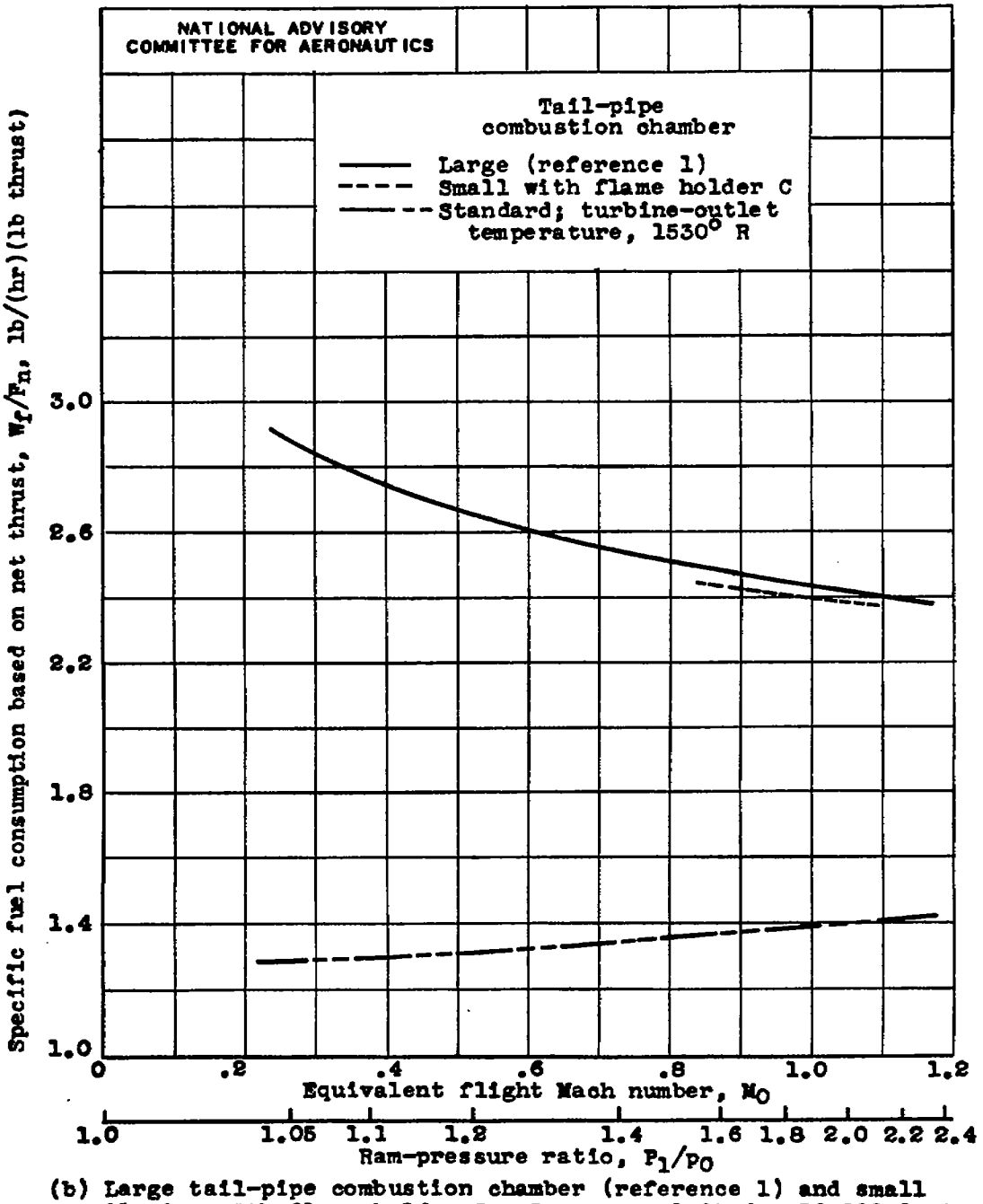

(b) Large tail-pipe combustion chamber (reference 1) and small tail pipe with flame holder C. Pressure altitude, 30,000 feet.

Figure 17.- Concluded. Relation between specific fuel consumption based on net thrust and equivalent flight Mach number of turbojet engine with standard tail pipe and with tail-pipe burning in modified tail pipes. Engine speed, 7600 rpm; 21-inch-diameter tail-pipe nozzle with tail-pipe burning; turbine-outlet temperature with tail-pipe burning, 1680° R.